New Phytologist

Research

The vacuolar Ca^{2+} transporter CATION EXCHANGER 2 regulates cytosolic calcium homeostasis, hypoxic signaling, and response to flooding in *Arabidopsis thaliana*

Arkadipta Bakshi[1]*, Won-Gyu Choi[2]*, Su-Hwa Kim[2] and Simon Gilroy[1]

[1]Department of Botany, University of Wisconsin, Birge Hall, 430 Lincoln Dr., Madison, WI 53706, USA; [2]Department of Biochemistry and Molecular Biology, 1664 N. Virginia St, Reno, NV 89557, USA

Author for correspondence:
Simon Gilroy
Email: sgilroy@wisc.edu

Received: *16 June 2023*
Accepted: *23 August 2023*

New Phytologist (2023)
doi: 10.1111/nph.19274

Key words: ACA1, calcium, CAX2, flooding, hypoxia, waterlogging.

Summary

- Flooding represents a major threat to global agricultural productivity and food security, but plants are capable of deploying a suite of adaptive responses that can lead to short- or longer-term survival to this stress. One cellular pathway thought to help coordinate these responses is via flooding-triggered Ca^{2+} signaling.
- We have mined publicly available transcriptomic data from Arabidopsis subjected to flooding or low oxygen stress to identify rapidly upregulated, Ca^{2+}-related transcripts. We then focused on transporters likely to modulate Ca^{2+} signals. Candidates emerging from this analysis included *AUTOINHIBITED Ca^{2+} ATPASE 1* and *CATION EXCHANGER 2*. We therefore assayed mutants in these genes for flooding sensitivity at levels from growth to patterns of gene expression and the kinetics of flooding-related Ca^{2+} changes.
- Knockout mutants in *CAX2* especially showed enhanced survival to soil waterlogging coupled with suppressed induction of many marker genes for hypoxic response and constitutive activation of others. *CAX2* mutants also generated larger and more sustained Ca^{2+} signals in response to both flooding and hypoxic challenges.
- CAX2 is a Ca^{2+} transporter located on the tonoplast, and so these results are consistent with an important role for vacuolar Ca^{2+} transport in the signaling systems that trigger flooding response.

Introduction

Environmental conditions, including soil compaction, intense microorganism activity, and flooding, can all lead to plants experiencing O_2-deficient surroundings, especially around the root system. These kinds of events can have devastating effects on plant productivity with flooding being one of the major factors in global crop losses (Fukao *et al.*, 2019). However, plants have evolved systems to sense and survive these naturally hypoxic conditions through processes such as shifting energy metabolism from aerobic to anaerobic pathways (reviewed in Bailey-Serres & Voesenek, 2010; Voesenek & Bailey-Serres, 2015).

The past few years have seen important advances in our understanding of the molecular details of how these plant flooding and hypoxia-related response systems are controlled. For example, low O_2-related signaling and response are known to involve the action of regulators ranging from hormones such as ethylene and gibberellin to a host of molecular players including ethylene response factors, acyl-CoA-binding proteins, MAP-kinases, SnRK1 kinase, the N-end protein degradation pathway, monomeric G-proteins, reactive oxygen species (ROS) and NO (reviewed in Bailey-Serres & Chang, 2005; Bailey-Serres & Voesenek, 2008; Sasidharan *et al.*, 2018; Schmidt *et al.*, 2018; Fukao *et al.*, 2019). However, despite these accumulating insights into how flooding response is controlled, precisely how plants monitor their anaerobic status and then integrate the network of cellular signals that control adaptive responses remains incompletely understood.

In addition to the signaling pathways outlined above, plants are thought to use Ca^{2+} as a second messenger to transduce hypoxic and flooding-related information. For example, Ca^{2+} changes have been linked to the low oxygen-triggered induction of genes such as *ALCOHOL DEHYDROGENASE 1* (*ADH1*), *SUCROSE SYNTHASE*, *HEMOGLOBIN* and *ALTERNATIVE OXIDASE 1a* (e.g., Subbaiah *et al.*, 1994a,b; Sedbrook *et al.*, 1996; Chung & Ferl, 1999; Tsuji *et al.*, 2000). Low O_2 is also known to increase Ca^{2+} influx into maize roots (Subbaiah *et al.*, 1994b) and anoxia-induced elevation in cytosolic Ca^{2+} has been observed in an array of plant samples ranging from cells of maize, rice, and wheat (Subbaiah *et al.*, 1994b, 1998; Yemelyanov *et al.*, 2011) to Arabidopsis seedlings (Sedbrook *et al.*, 1996). Indeed, plasma membrane ion channels have even been proposed as candidate O_2 sensors (Wang *et al.*, 2017). In addition, a Ca^{2+} increase triggered in response to the falling cellular energy charge

*These authors contributed equally to this work.

that accompanies lowered O_2 availability has been suggested as a possible general mechanism to trigger responses to hypoxic stress (Igamberdiev & Hill, 2018).

Waterlogging in Arabidopsis has been correlated with suppressed expression of the Ca^{2+}-ATPase *ACA8*, the Ca^{2+}/H^+ antiporters *CAX4,* and of *CCX5*, a member of the Calcium Cation eXchanger super-family (Wang *et al.*, 2016). Mutants in *CCX5* showed hypersensitivity to 3 wk of flooding stress leading to the suggestion that this transporter maintains normal cellular Ca^{2+} homeostasis under these conditions. Furthermore, knockout of *CAX1* has recently been shown to yield tolerance to the stresses associated with recovery from submergence and anoxic treatment (Yang *et al.*, 2022). In addition, Ca^{2+} response elements such as CALMODULIN-LIKE 38 (CML38) in Arabidopsis and CALCINEURIN-B INTERACTING PROTEIN KINASE 15 (OsCPIK15) in rice have been linked to hypoxic responses (Lee *et al.*, 2009; Meyer *et al.*, 2010; Lokdarshi *et al.*, 2016). However, the systems generating hypoxia-related Ca^{2+} signals and associated Ca^{2+}-dependent response elements still remain largely undefined.

To help identify candidates of this Ca^{2+}-related hypoxia and flooding signaling network, we have used analysis of publicly available transcriptome responses of Arabidopsis plants exposed to low O_2 to target hypoxia- and flooding-induced, Ca^{2+}-related genes. This analysis highlights the expression of the vacuolar Ca^{2+} transporter *CAX2* as being linked to flooding and hypoxia-related signaling. We further report that mutants in *CAX2* show elevated flooding and hypoxia-triggered Ca^{2+} signaling and altered molecular responses to these stresses. Mutants in *CAX2* also show enhanced resistance to waterlogging of the soil. These observations suggest that CAX2 is an important component regulating the activity of the flooding response network, likely through its effects on the flooding-induced Ca^{2+}-signaling network.

Materials and Methods

Plant growth and transformation

Seeds of *Arabidopsis thaliana* (L.) Heynh. ecotype Col-0 were obtained from Lehle seeds (Round Rock, TX, USA). Seeds of *cax2-2* (Supporting Information Fig. S1; Pittman *et al.*, 2004) were a kind gift from Dr Kendal Hirschi (Baylor School of Medicine, Houston, TX, USA). *cax2-3* (Fig. S1; Salk_042383C) and *aca1-1* (Salk_206556C; Fig. S1) were obtained from the Arabidopsis Biological Resource Center (The Ohio State University, Columbus, OH, USA). R-GECO1 expressing plants (Keinath *et al.*, 2015) were a kind gift from Drs Rainer Waadt and Melanie Krebs (University of Heidelberg, Heidelberg, Germany). Agrobacterium-mediated transformation with YCNano-65/pEarleyGage100 and selection of transformed lines was as described in Choi *et al.* (2014).

Hypoxia, flooding, and inhibitor treatments

Plant waterlogging in pots and measurement of rosette growth characteristics was performed as described in Bakshi & Gilroy (2023). For soil waterlogging treatment, 17 pots per tray for control (untreated) and waterlogged treatments were prepared. Pot inserts were equally filled to the top with soil, compressed by *c.* 1 cm, and arranged in the tray randomly for different genotypes. An empty pot was placed in the 18th spot to both monitor and maintain the water table during the experiment. The top of every pot was carefully covered with a black cloth (with a slit to its middle) that fitted around the seedling covering the soil (Fig. S2). Plants were then grown under short-day conditions (16 h : 8 h, dark : light at *c.* 100 µmol/m^2/s light intensity). For waterlogging, the tray was completely filled with water through the open 18th spot to the soil level, and this water table was maintained throughout the flooding treatment. The nonflooded control tray was watered to 1 cm standing water through the empty 18th spot. This level was replenished throughout the duration of the experiment each time the water level fell to zero (Fig. S2).

For microscopy, Arabidopsis seedlings were grown for 7–10 d on a thin layer of 0.8% v/v Phytagel (Sigma) made up in ½ strength Linsmaier and Skoog medium (Phytotech Labs, Lenexa, KS, USA) containing 10 mM sucrose according to Choi *et al.* (2014). For flooding treatment on the microscope, the specimen was immersed in 5 ml of medium that had been deoxygenated by bubbling with N_2(g) for 10 min before use. Controls used a medium similarly bubbled with air.

For anoxic and hypoxic treatments, a custom microscope chamber was constructed from Plexiglass (Fig. S3) where the bottom of the chamber was made up of the coverslip with the growth gel and plant on it (allowing imaging from below using an inverted confocal microscope) and top of the chamber was made by a separate coverslip, allowing imaging from above with, for example an AxioZoom fluorescence microscope (Carl Zeiss Inc., Thornwood, NY, USA). Both coverslips were sealed in place by silicone vacuum grease (Dow Corning, Midland, MI, USA). The chamber (total internal volume *c.* 2 ml, airspace *c.* 500 µl) had a gas inlet port and outlet port to allow exchange of the atmosphere over the plant. Humidified (bubbled through water) N_2(g) or air was then perfused into the chamber as needed. The chamber outlet was sent to a DrDAQ O_2 sensor (Pico Technology, St Neots, UK), allowing for the continuous measurement of the changes in O_2 levels in the chamber, which exchanged with the incoming gasses over *c.* 2 s.

Imaging of Ca^{2+} changes

Two different GFP-based Ca^{2+} reporters, R-GECO1 and YCNano-65, were used to image Ca^{2+} changes. These sensors use different detection technologies. R-GECO is an intensiometric reporter based on the cpmApple fluorescent protein (Zhao *et al.*, 2011), whereas YCNano-65 is a Förster resonance Energy Transfer (FRET)-based sensor built around eCyan Fluorescent Protein and cpVenus fluorescent proteins (Horikawa *et al.*, 2010). Therefore, when these two reporters are in agreement on the dynamics of any Ca^{2+} change, it increases the confidence with which those patterns can be described.

R-GECO-1 was monitored using an AxioZoom V16 fluorescence stereo microscope equipped with a PlanNeoFluar Z 1.0×/

0.25 lens, using 545/25 nm excitation, a 570 nm dichroic mirror, and 605/70 nm emission. Ratio imaging of YCNano-65 expressing plants on the AxioZoom was performed using a PlanNeoFluar Z 1.0×/0.25 lens, 440/40 nm excitation, a 495 nm dichroic mirror, and dual emissions (475/20 nm for CFP and 540/30 nm for cpVenus) measured using the W-view Gemini Image beam splitter and a Hamamatsu ORCA-Flash4.0 V2 Plus sCMOS digital camera (Hamamatsu Photonics Inc., San Jose, CA, USA). Ratio confocal images were taken with an LSM710 Meta laser scanning confocal microscope (Zeiss) with a Plan-Neofluar 10×/0.3 or 20×/0.75 Plan-Apochromat objective as described previously (Choi *et al.*, 2014) using the 458 nm line of an argon laser and emission wavelengths (CFP: 462–505 nm, cpVenus/FRET: 526–537 nm) monitored with a 458 nm primary dichroic mirror and the confocal system's spectral Meta-detector. Analysis of Ca^{2+} levels using ratio analysis (YFP emission/CFP emission) for both the AxioZoom and confocal imaging systems was performed using ImageJ (Schindelin *et al.*, 2012) as described previously (Choi *et al.*, 2014).

Quantification of chlorophyll, carotenoid, anthocyanin, and L-lactate content

Pigment levels were measured as described previously (Bakshi & Gilroy, 2023). For determination of L-lactate levels, 100 mg of Arabidopsis shoot tissue samples were extracted in ice-cold 3.5% (v/v) perchloric acid. This buffer was then neutralized with 2 M KOH, 150 mM HEPES, and 10 mM KCl to bring the pH to 7. These samples were frozen and thawed (to precipitate potassium perchlorate salts) and then centrifuged at *c.* 18 000 ***g*** for 3 min at 4°C. The supernatant was used to assay lactate concentration by the lactate dehydrogenase (LDH) method of Bergmeyer & Bernt (1974).

RNA isolation and real-time qRT-PCR

Total RNA was isolated from 100 to 150 mg of plant tissues using the Spectrum Plant Total RNA kit (Sigma) according to the manufacturer's directions. Real-time qPCR was performed as described in Hilleary *et al.* (2020) and Schmittgen & Livak (2008). Transcript levels were normalized to *UBQ10*, and the qPCR primers used are described in Table S1.

Analysis of publicly available transcriptome data

Table S2 summarizes the publicly available transcriptome datasets from Arabidopsis plants subjected to flooding and hypoxia treatments that were analyzed for candidate Ca^{2+} signaling genes. We used the authors' published analyses of significantly differentially expressed genes and filtered this list for those falling into 'Bin 30.30, signaling.calcium' using MapMan (Thimm *et al.*, 2004). Genes showing increases in expression would provide strong candidates for functional characterization by our planned knockout/knockdown approach. Therefore, we further filtered the list to those showing a ≥ 1.5-fold upregulation in expression in three or more of the studies.

Results

Hypoxic stress rapidly modulates Ca^{2+} levels in roots

We first asked where flooding-induced Ca^{2+} changes were most evident in the plant. We took advantage of the ability to image whole seedlings that are ubiquitously expressing the R-GECO1 fluorescent protein-based Ca^{2+} biosensor. R-GECO1 fluorescence becomes brighter as cellular Ca^{2+} levels rise providing a qualitative overview of their spatial and temporal dynamics.

To elicit a large flooding/hypoxic response, we compared plants flooded with medium that had been deoxygenated (by bubbling with N_2 gas) vs well-oxygenated media that had been similarly treated but with air. Fig. 1 and Videos S1–S4 show that in response to this flooding/hypoxic stimulus, we observed Ca^{2+} changes at the root apex, whereas flooding with a well-aerated medium did not trigger equivalent events. Calcium signals were not readily evident in the mature parts of the root or the rosette. However, large Ca^{2+} increases could subsequently be induced in the rosettes of these same plants by wounding, a stimulus well-characterized as triggering Ca^{2+} changes within the aerial parts of the plant (Toyota *et al.*, 2018). This observation suggests that although the plants were capable of generating Ca^{2+} signals in their aerial tissues, in the context of our flooding treatments (i.e. plants grown on plates on solid gel medium flooded with a layer of liquid medium), large Ca^{2+} changes were only detectable in the root apex.

Fig. 1 and Video S1 show a rapid change in Ca^{2+} at the very apex of the root but the root cap is poorly resolved by R-GECO imaging due to the very high expression of this reporter in these tissues. These changes were however resolvable using confocal imaging of the root apex of plants expressing an alternative Ca^{2+} reporter (YCNano-65; Horikawa *et al.*, 2010). This imaging approach revealed that the Ca^{2+} signals at the very tip of the root started in the root cap columella within seconds of flooding (Fig. S4). Taken together, these imaging results suggested to us that concentrating on root responses would provide a productive focus for our subsequent analyses of the Ca^{2+} response machinery to flooding stimuli.

Hypoxic stress rapidly modulates the transcription of a Ca^{2+}-related network

As described in the introduction, a hypoxia/flooding-related Ca^{2+} signaling network is thought to modulate transcriptional responses to this stress. Therefore, we used MapMan (Thimm *et al.*, 2004) to analyze the transcriptomics data from published Arabidopsis flooding and hypoxia experimentation (studies analyzed are summarized in Table S2). We filtered these data for Ca^{2+}-signaling-related genes showing ≥ 1.5-fold significant increases in the expression in three or more of the transcriptome studies. We then used the eFP browser (Toufighi *et al.*, 2005) and Genevestigator (McCormack *et al.*, 2005) to further focus our analysis on genes showing detectable expression in the root. As initial inspection showed there was a high representation of calmodulin-like (CML) genes in this analysis, we included the three other CMLs in the Arabidopsis genome that were not

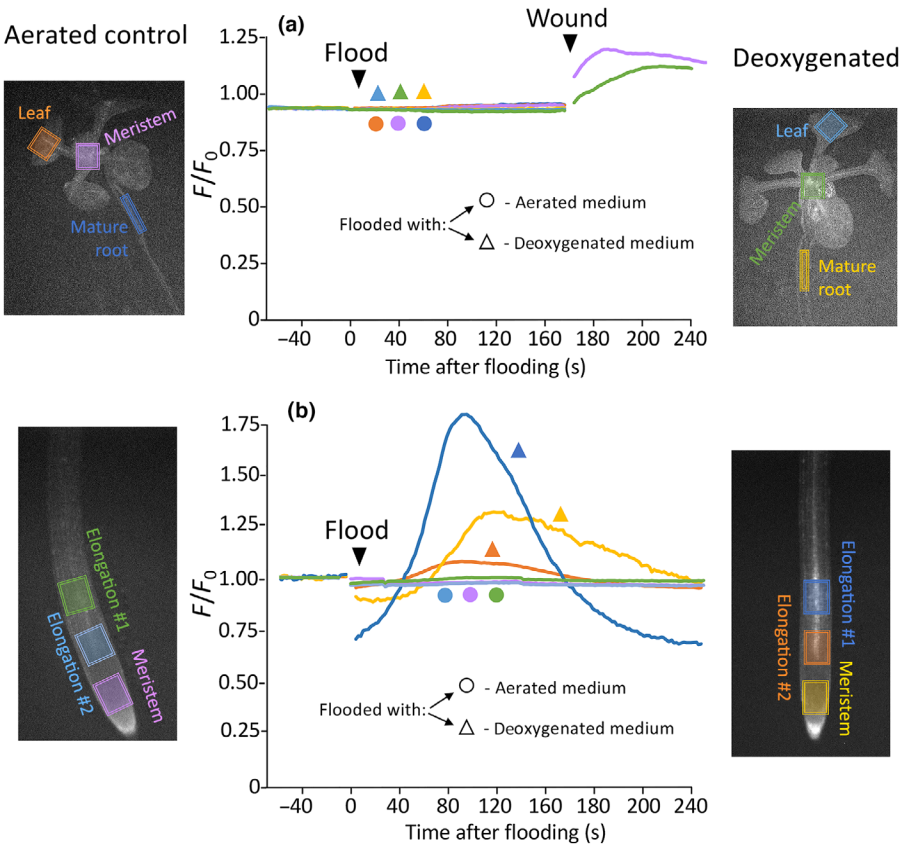

Fig. 1 Flooding triggers changes in Ca^{2+} levels in wild-type plants of *Arabidopsis thaliana*. Seven to 10-d-old Col-0 plants expressing the fluorescent protein-based Ca^{2+} biosensor R-GECO1 were flooded with either well-aerated or deoxygenated medium (bubbled with air or N_2 gas respectively). Shoot (a) and root (b) Ca^{2+} levels were monitored using R-GECO1 fluorescence (*F*) extracted from the indicated regions in the inset images using ImageJ. Measurements have been normalized to the average fluorescence for 60 s before flooding (F_0). As a positive control for responsiveness of the plants, a leaf was mechanically wounded at the indicated time by cutting through the petiole using scissors. This technique is well characterized to trigger wound-induced Ca^{2+} increases throughout the rosette (Toyota *et al.*, 2018). Results representative of $n \geq 5$ replicates. These same data are shown in Supporting Information Videos S1–S4.

highlighted in this initial transcriptomics screen but that also showed root expression in the eFP browser (CMLs 2, 6 and 23).

Fig. 2 shows that this analysis led to the identification of 32 Ca^{2+}-related, hypoxia-induced candidates that included 16 calmodulin-like proteins, 4 calcium-dependent protein kinases, 6 calmodulin-binding proteins, and 2 Ca^{2+} transporters (Fig. 2a,c). Using these genes to query the gene list annotation and analysis tool Metascape (Zhou *et al.*, 2019) revealed that in addition to the expected groupings of genes related to the factors underlying the screening approach (i.e. hypoxia and Ca^{2+} signaling), this list of genes also showed enrichment for those related to ketone metabolism, protein kinase activity, cation transport and pathogen response (Fig. 2f).

As our list of candidate genes was drawn from analysis of the literature, we next asked which of them continued to show the expected transcriptional upregulation in our specific flooding experimental setup. First, to validate that our flooding assay yielded a canonical transcriptional response, we used real-time qPCR to monitor expression of the classic hypoxic response marker *ADH1*. Our transcriptomics mining analysis also suggested that *CML5* should show no transcriptional response to flooding stress, providing us with a negative control. Both *ADH1* and *CML5* showed these expected responses (Fig. 2b,c; Table S3). Using this same flooding/qPCR approach, we were able to demonstrate that 28 of our 32 candidates showed significant accumulation of transcript in response to flooding in our experimental system (Fig. 2c–e; Table S3).

Previous studies on cell cultures and seedlings used the sensitivity of the induction of markers such as *ADH1* to pretreatment with pharmacological inhibitors of Ca^{2+} channels to infer the close link between low O_2-induced Ca^{2+} signals and Ca^{2+}-dependent transcriptional regulation (e.g., Subbaiah *et al.*, 1994a; Sedbrook *et al.*, 1996; Chung & Ferl, 1999). Although such a pharmacological approach has the potential for off-target side effects (e.g., Lewis & Spalding, 1998), it provided us with a useful starting point to characterize our Ca^{2+}-related transcriptional network relative to these previous reports. La^{3+} is a putative plasma membrane Ca^{2+} channel blocker widely used to inhibit Ca^{2+} influx into plant cells and that is effective in roots (e.g., Choi *et al.*, 2014). We therefore first used qPCR analysis to establish that the flooding-associated induction of *ADH1* was indeed inhibited by La^{3+} pretreatment in our flooding experiments (Fig. 2b). We then surveyed how a similar La^{3+} treatment affected our Ca^{2+} response network genes. La^{3+} pretreatment inhibited the flooding-triggered induction of only a subset of our 32 candidate genes. Thus, the hypoxia-increased transcript levels of 16 genes were inhibited under these conditions, 12 were unaffected, and four were induced (Fig. 2c; Table S3). Assuming these effects on transcription are mediated through La^{3+}-related blockage of a flooding-triggered Ca^{2+} increase, these results suggest *c.* 50% of the flooding stress-induced Ca^{2+} response network that we have identified is induced by Ca^{2+} changes, *c.* 12% is repressed by these signals and the transcription of the remaining genes is unaffected by hypoxia-triggered Ca^{2+} changes.

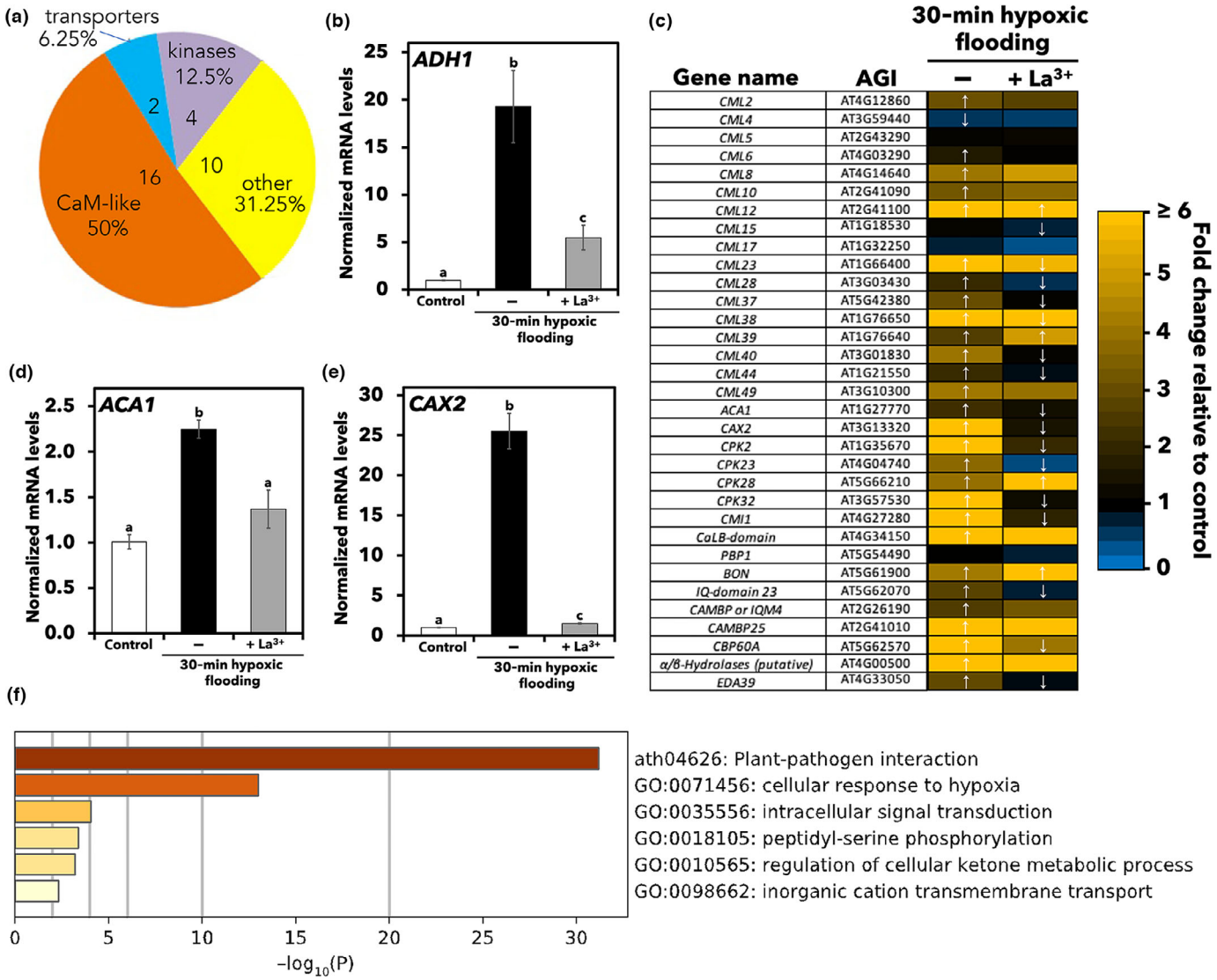

Fig. 2 Hypoxia stress leads to altered transcription of a Ca^{2+}-related gene network in *Arabidopsis thaliana*. (a) Publicly available transcriptome-level data on hypoxic response filtered for Ca^{2+}-related, root-expressed genes that were significantly up-regulated within 12 h of hypoxia. (b) Real-time quantitative polymerase chain reaction (qPCR) analysis of *ADH1* expression in response to 30-min hypoxic flooding with or without pretreatment with 25 μM $LaCl_3$. (c) Response in expression of all 32 candidate genes in (a). The heat map was generated using mean values of real-time qPCR data of four independent biological replicates (see Supporting Information Table S3 for quantitative data). ∧, significantly upregulated; ∨, significantly downregulated; $P < 0.05$ one-way ANOVA and Benjamini and Hochberg correction for multiple comparisons. (d, e) Real-time qPCR analysis of *ACA1* and *CAX2* expression in response to 30-min hypoxic flooding with or without pretreatment with 25 μM $LaCl_3$ (quantitative data redrawn from the heatmap in c and Table S3). (f) Functional enrichment of Gene Ontologies analyzed using Metascape (Zhou *et al*., 2019). Treatments: control, no hypoxic flooding; 30-min hypoxic flooding, 30 min of treatment imposed with deoxygenated plant growth medium; + La^{3+}, pretreatment with 25 μM La^{3+} 1 h before 30-min hypoxia treatment with deoxygenated medium. Bars sharing the same letters in (b, d and e) denote treatments that are not significantly different from each other, $P < 0.05$, one-way ANOVA with Benjamini and Hochberg test for multiple comparisons. Results are mean ± SEM. *ADH1*, *ALCOHOL DEHYDROGENASE 1*; *ACA1*, *AUTOINHIBITED Ca^{2+} ATPASE 1*; *CAX2*, *CATION EXCHANGER 2*.

Of all the candidate genes in the Ca^{2+} response network described above, the two Ca^{2+} transporters, *CAX2* and *ACA1*, would be predicted to most directly affect the dynamics of Ca^{2+} signals. Both encode proteins predicted to move Ca^{2+} from the cytosol into an intracellular store – the vacuole for CAX2 (Pittman *et al*., 2004) and ER for ACA1 (Ishka *et al*., 2021). Thus, both would be predicted to play roles in limiting the magnitude or duration of any cytosolic Ca^{2+} signal. Therefore, we next focused on investigating whether *CAX2* or *ACA1* play functional roles in how Arabidopsis plants react to flooding and whether they potentially act by altering the dynamics of the Ca^{2+} signals generated by this stress.

Mutants in *CAX2* and *ACA1* show resistance to flooding stress

We obtained mutants in *CAX2* and *ACA1* (*cax2-2* and *aca1-1*; Fig. S1a), and qPCR analysis indicated that these mutant alleles

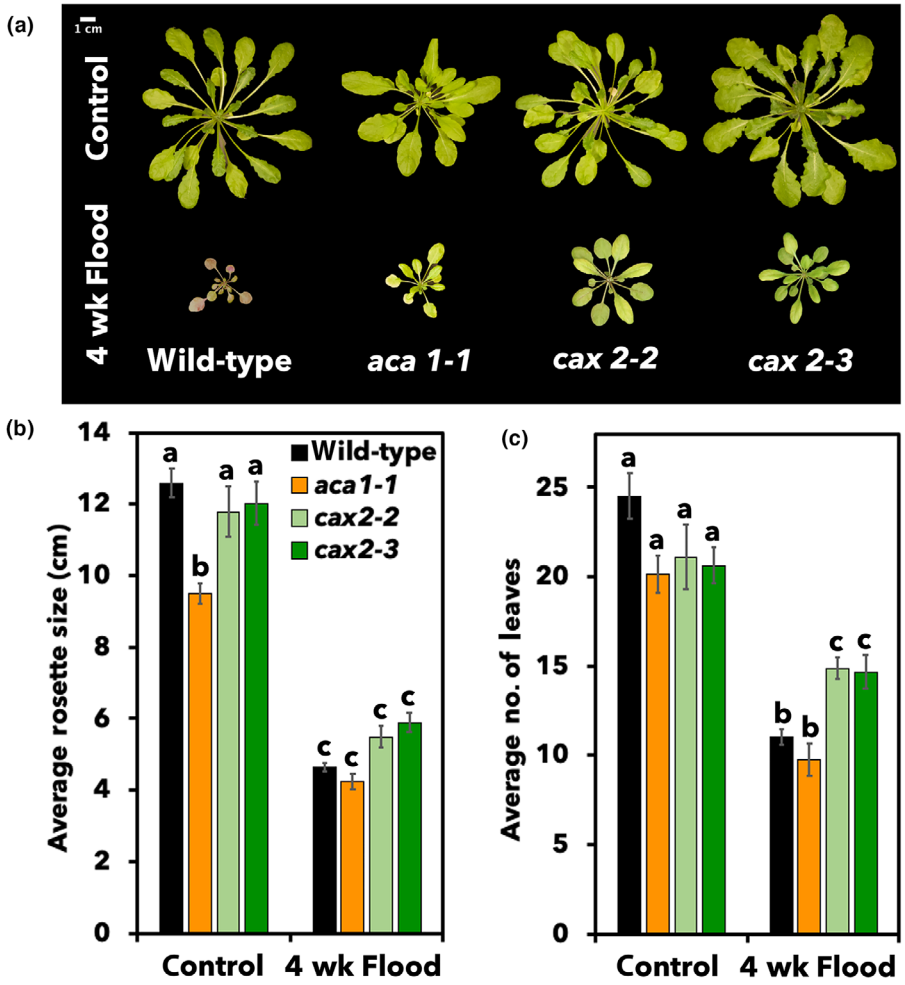

Fig. 3 Vegetative growth of *cax2*, *aca1* mutants, and wild-type *Arabidopsis thaliana* plants is altered in response to flooding. (a) Images of wild-type, *aca1-1*, *cax2-2*, and *cax2-3* plants after 4 wk of waterlogging or of the untreated (control) plants, (b) rosette size (diameter) and (c) number of leaves were calculated using ImageJ. Results represent mean ± SE of 8–12 biological replicates from four independent experiments. Data were analyzed using one-way ANOVA and Tukey's multiple comparisons test. For each graph, bars sharing the same letters are not significantly different from each other ($P < 0.05$).

(and a second allele *cax2-3*, to be described later) were severe knockdowns/knockouts (Fig. S1b). Fig. 3 shows that when grown without a flooding stimulus *cax2-2* plants did not show any obvious vegetative growth phenotype (Fig. 3a), whereas *aca1-1* exhibited a small but significant (*c.* 25%) reduction in rosette size (Fig. 3a,b).

To target root-related flooding events we focused on how these plants responded to continuous waterlogging of the soil, that is where the floodwater level is maintained at the soil surface but does not submerge the aerial parts of the plant. When 3-wk-old plants were subjected to a subsequent 4 wk of such flooding stress, wild-type plants exhibited a significant reduction in rosette growth, leaf production, chlorophyll levels and carotenoid content (Figs 3b,c, 4a,b) and an increase in the levels of the stress pigment (Li *et al.*, 2016) anthocyanin (Fig. 4c). Although the response of *aca1-1* resembled wild-type in these assays, *cax2-2* plants showed characteristics suggestive of flood tolerance. Thus, although wild-type, *aca1-1* and *cax2-2* all displayed a significant decrease in their rosette size and leaf production in response to flooding, *cax2-2* plants made a rosette with significantly more leaves than the other two genotypes (Fig. 3c). Similarly, post-flooding, chlorophyll content decreased to a similar extent in wild-type and *aca1-1*, whereas *cax2-2* showed no significant change (Fig. 4a). We also observed an *c.* 55–60% lowering in foliar carotenoid concentrations in flood-stressed wild-type and *aca1-1* plants, whereas again *cax2-2* plants showed no significant change (Fig. 4b). Waterlogging led to an *c.* 17-fold increase in anthocyanin accumulation in the wild-type plants. *aca1-1* similarly showed elevated anthocyanin to levels that were not significantly different to wild-type, whereas anthocyanin levels in *cax2-2* rose by only *c.* fivefold (Fig. 4c).

We next used qPCR to examine the transcript abundance of genes known to show changes in expression upon hypoxic stress: *PYRUVATE DECARBOXYLASE 1* (*PDC1*), *ADH1* (Chung & Ferl, 1999; Mithran *et al.*, 2014), *HEAT SHOCK PROTEIN 70* (*HSP70*; Lin *et al.*, 2001; Pucciariello *et al.*, 2012; Choi *et al.*, 2019) and *FAD-LINKED OXIDOREDUCTASE 1* (*FOX1*; Boudsocq & Sheen, 2010). Fig. 5a–d shows that flooding stress resulted in a significant increase in all of these molecular markers in wild-type plants. Induction of these genes also occurred in *aca1-1* but was significantly lower than wild-type plants for all except for *HSP70*. By contrast, none of these markers showed significant induction by flooding in *cax2-2* mutant plants.

To more robustly link the flooding tolerance phenotypes seen in *cax2-2* to lesion in the *CAX2* gene, we confirmed the phenotyping described above with an independent allele (*cax2-3*, Fig. S1a). This second allele showed reactions to flooding that were identical to *cax2-2* (Figs 3–5), strongly connecting these

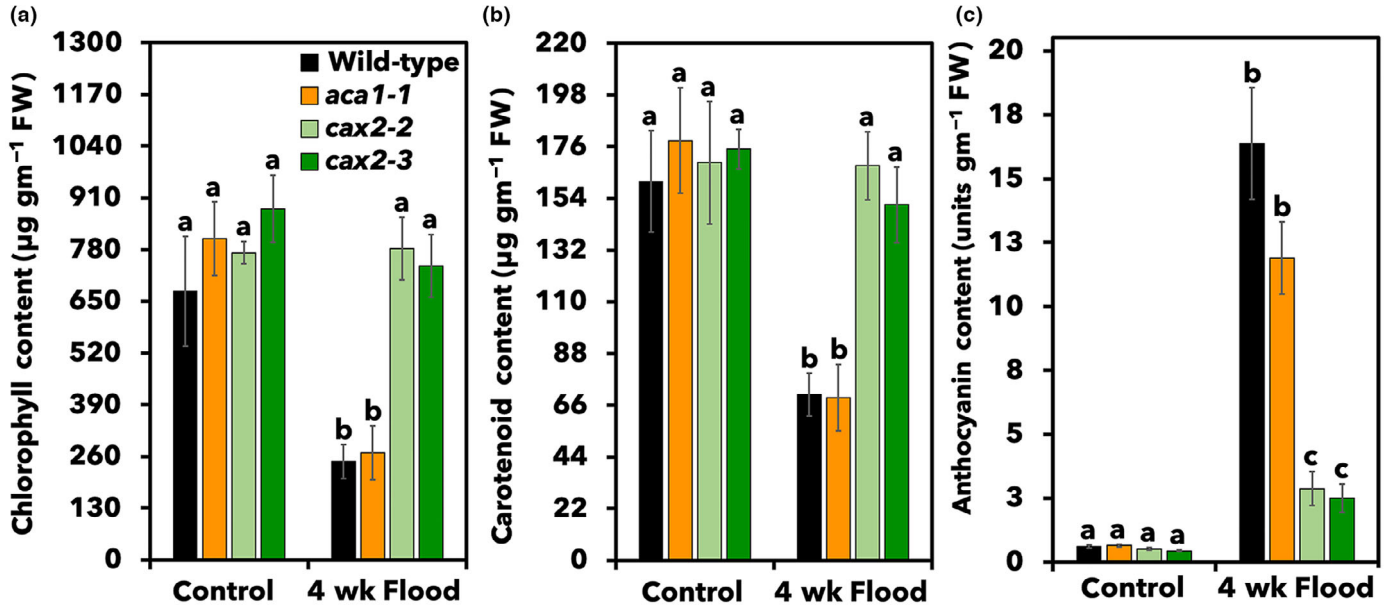

Fig. 4 Pigment levels in *Arabidopsis thaliana* wild-type and mutants in *CAX2* and *ACA1* are altered in response to flooding stress. Shoot tissue samples were harvested to determine the total chlorophyll (a), carotenoid (b), and anthocyanin (c) contents from plants experiencing waterlogging of the soil for 4 wk vs unflooded controls. Data represent mean ± SE for five to eight independent biological replicates. Data were analyzed using one-way ANOVA and Tukey's multiple comparisons test. In each panel, bars sharing, the same letters are not significantly different ($P < 0.05$). *ACA1*, *AUTOINHIBITED* Ca^{2+} *ATPASE 1*; *CAX2*, *CATION EXCHANGER 2*.

phenotypes to effects from disruption of expression of the *CAX2* gene. As *cax2* mutants showed a broader suite of flooding resistance phenotypes than those in *ACA1*, we focused our further analyses on how *CAX2* might play a role in the Arabidopsis Ca^{2+}-related flood signaling and response network.

cax2 mutant plants exhibit tolerance to short-term flooding stress

The above data suggest CAX2 involvement in long-term responses to flooding. However, in the literature, Ca^{2+} signals and Ca^{2+}-responsive gene expression have largely been characterized in the initial events of hypoxic stress. Therefore, we examined the effect of short-term flooding on wild-type plants compared with both alleles of *CAX2* by subjecting 3-wk-old plants to 2 h of waterlogging conditions. As this short period of time is insufficient for large-scale changes in growth or pigment levels to become evident, we concentrated on following molecular markers of the hypoxic response and so expanded the panel of molecular markers to include two other genes linked to the Ca^{2+}-dependent hypoxic response pathway: *SUCROSE SYNTHASE 1* (*SUS1*; Santaniello *et al.*, 2014) and *NODULIN26-LIKE INTRINSIC PROTEIN 2;1* (*NIP2;1*; Choi & Roberts, 2007). The gene expression analysis in Fig. 6a–d shows a similar pattern of induction in the transcript levels of *PDC1*, *ADH1*, *HSP70,* and *FOX1* as seen in the long-term flooding response shown in Fig. 5. However, analysis of *SUS1* and *NIP2;1* showed that the *cax2* knockout plants expressed both of these genes at the levels seen in flooded wild-type whether this stress was present or not (Fig. 6e,f).

We also monitored the expression of *ACA1* and the other *CAX* family members in wild-type and *cax2* mutant plants under flooding stress. *CAX4* transcript levels were unaltered in the *cax2* background and showed no change in expression upon flooding (Fig. S5). Although not highlighted in our original bioinformatics analyses, we found that *CAX3* behaved similarly to flooding response genes such as *ADH1* (Figs 5, 6) with basal expression in the *cax2* mutants resembling wild-type but loss of induction by flooding in the *cax2* background. *CAX1* was upregulated in *cax2* by *c.* twofold, but this increase was not responsive to flooding stress. For *ACA1*, basal expression was unchanged in *cax2* but its induction upon flooding was increased from *c.* 2.4-fold in wild-type to 3.4- to 3.8-fold in the *cax2* backgrounds (Fig. S5).

Lastly, we assayed expression of representative genes from the Ca^{2+}-related network outlined in Fig. 2 to ask how they responded in the *cax2* background: *CML10* was chosen as a member of the group where induction by flooding is not affected by La^{3+} treatment (i.e. putatively Ca^{2+}-independent upregulation); *CML23* (putative Ca^{2+}-dependent induction); and *BON1* (putative Ca^{2+} repressed response). Fig. 6g–i shows that basal *CML10* and *CML23* expression was unaltered in the *cax2* background whereas *BON1* showed an *c.* 1.7-fold increase that was not responsive to flooding. Flooding induction of *CML10* was no longer seen in *cax2* plants, mirroring the patterns of response seen in genes such as *ADH1*, whereas flooding induction of *CML23* was increased in the *cax2* mutants.

cax2 mutant plants do not accumulate lactic acid in response to flooding stress

When plants are exposed to flooding, one of their survival strategies is to switch from aerobic to anaerobic respiratory pathways to cope with the low availability of dissolved O_2. Lactic acid is produced as

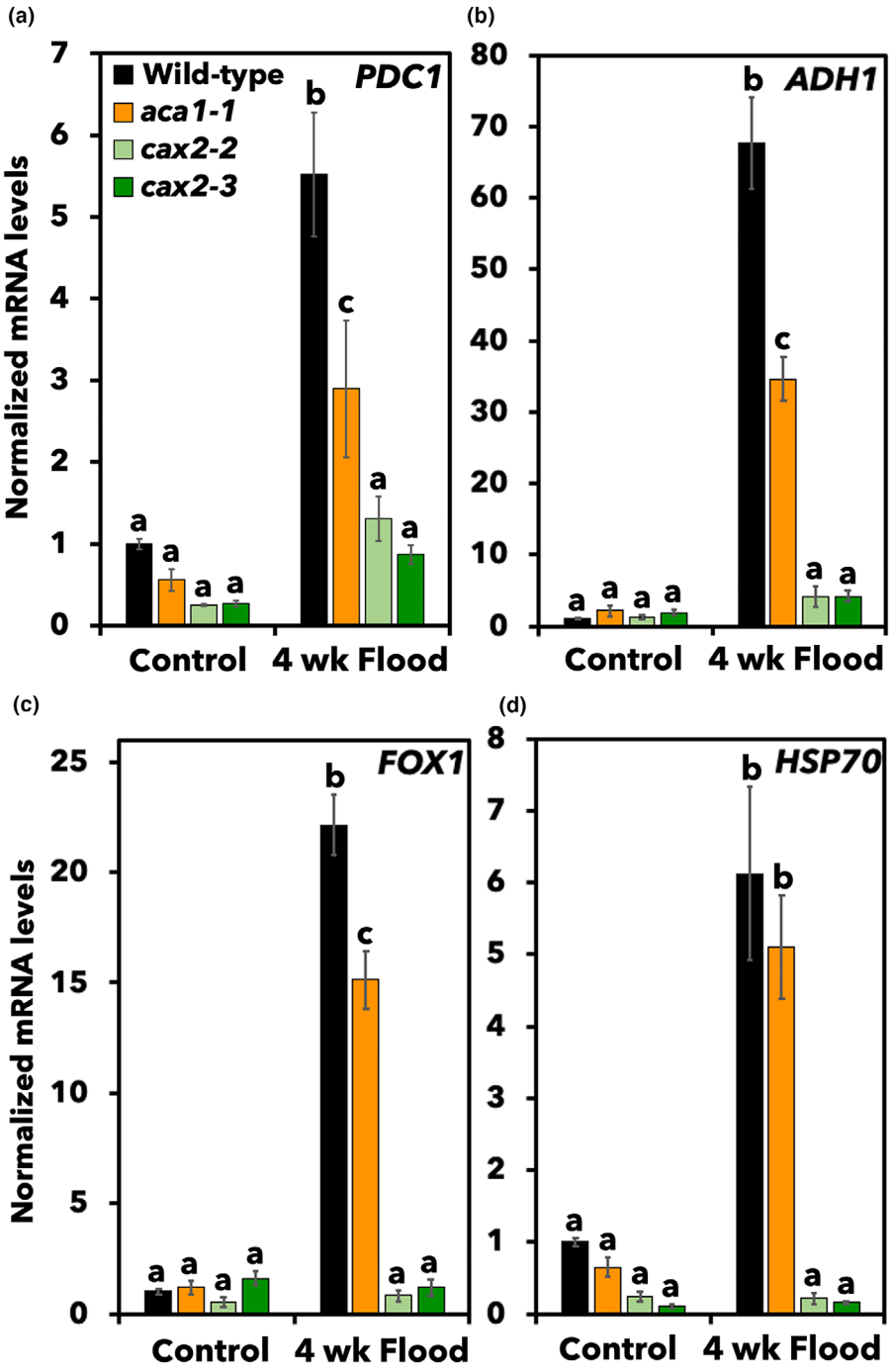

Fig. 5 Flooding triggers differential changes in gene expression patterns in *Arabidopsis thaliana* wild-type and mutants in *CAX2* and *ACA1*. The transcript levels of the flood/low-oxygen responsive genes (a) *PDC1*, (b) *ADH1*, (c) *FOX1,* and (d) *HSP70* were analyzed with real-time quantitative polymerase chain reaction (qPCR) after 4 wk of waterlogging conditions compared with unflooded controls. Data represent mean ± SE for three to four independent biological replicates, normalized to levels of the transcript in untreated wild-type plants. In each panel, bars sharing the same letters are not significantly different (one-way ANOVA and Tukey's multiple comparisons test, $P < 0.05$). *ACA1*, *AUTOINHIBITED* Ca^{2+} *ATPASE 1*; *CAX2*, *CATION EXCHANGER 2*; *PDC1*, *PYRUVATE DECARBOXYLASE 1*; *ADH1*, *ALCOHOL DEHYDROGENASE 1*; *FOX1*, *FAD-LINKED OXIDOREDUCTASE 1*; *HSP70*, *HEAT SHOCK PROTEIN 70*.

one of the products of such anaerobic biochemistry (Greenway & Gibbs, 2003). *NIP2;1* is a lactate channel closely linked to modulating lactate accumulation during hypoxic response in Arabidopsis (Choi & Roberts, 2007; Beamer *et al.*, 2021). The constitutive upregulation of *NIP2;1* in the *cax2* mutant backgrounds therefore suggested to us a possible shift in anaerobic metabolism linked to lactate production. Indeed, under nonflooded conditions, both wild-type and *cax2* plants displayed similarly low levels of lactate accumulation. However, in response to 2 h of waterlogging, the significant accumulation of L-lactate seen in wild-type plants was not evident in the *cax2* mutants (Fig. 6j).

Loss of function of *CAX2* alters the expression of enzymes involved in pyruvate and lactate metabolism

In addition to lactate production, some of the other pathways contributing to anaerobic metabolism are summarized in Fig. 7. Thus, in Arabidopsis, L-lactate is produced from pyruvate via LACTATE DEHYDROGENASE 1 (LDH1; Dolferus *et al.*, 2008). The lactate produced can be exported (NIP2;1) or metabolized further, such as being recycled back into the pyruvate pool by the action of peroxisomal GLYCOLATE OXIDASE 3 (GOX3; Engqvist *et al.*, 2015). In addition, ethanolic fermentation mediated by

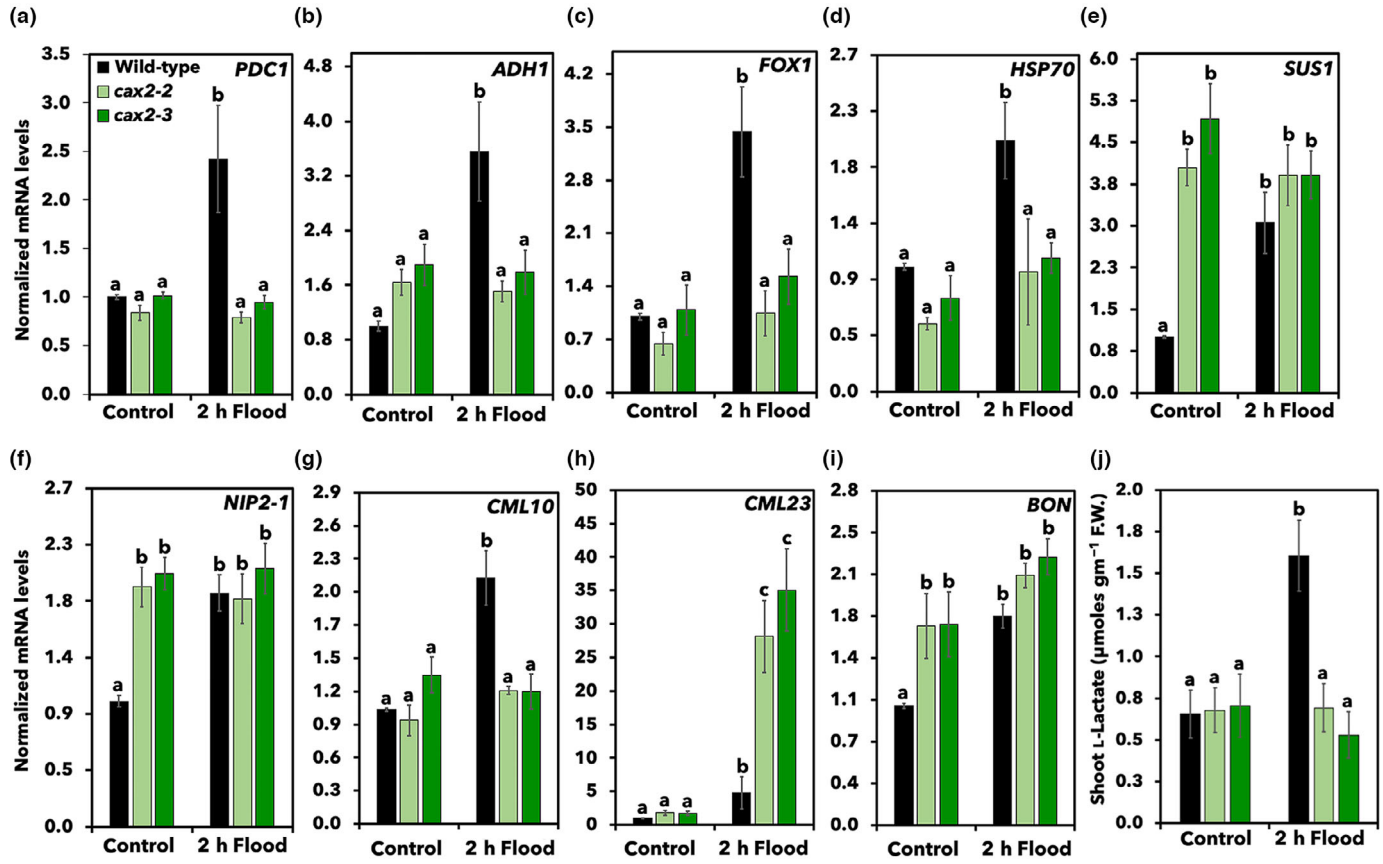

Fig. 6 *Arabidopsis thaliana cax2* displays tolerance toward short-term flooding stimuli. (a–i) Transcript levels of flood, low-oxygen, and calcium-responsive genes in wild-type, *cax2-2,* and *cax2-3* mutant plants in response to 2 h waterlogging stress. *PDC1*, *PYRUVATE DECARBOXYLASE 1*; *ADH1*, *ALCOHOL DEHYDROGENASE 1*; *FOX1*, *FAD-LINKED OXIDOREDUCTASE 1*; *HSP70*, *HEAT SHOCK PROTEIN 70*; *SUS1*, *SUCROSE SYNTHASE 1*; *NIP2;1*, *NODULIN26-LIKE INTRINSIC PROTEIN 2;1*; *CML10*, *CALMODULIN LIKE 10*; *CML23*, *CALMODULIN LIKE 23*; and *BON1*, *BONZAI 1*. (j) Lactic acid levels in response to 2 h waterlogging stress. Bars sharing the same letters are not significantly different from each other (one-way ANOVA and Tukey's multiple comparisons test, $P < 0.05$). Data are the average ± SE for 3–4 (a–i) and six (j) independent biological replicates.

PDC1 and ADH1 sequentially converts pyruvate to acetaldehyde and finally to ethanol. Pyruvate can also be converted to alanine by ALANINE AMINOTRANSFERASE 1 (AlaAT1; Miyashita *et al.*, 2007). Transcription of all of these enzymes is induced by flooding in wild-type plants (Fig. 7). In the *cax2* background, *LDH1* and *AlaAT1* expression behaved similarly to wild-type with no change in basal expression and upregulation by *c.* fivefold under 2 h flooding stress (Fig. 7a–c). This is in contrast to flooding-triggered induction in expression of the alcoholic fermentation pathway enzymes *ADH1* and *PDC1* which is repressed in the *cax2* background (Fig. 6a,b). *GOX3* expression resembled that of *NIP2;1* being constitutively elevated in *cax2* to the levels seen upon flooding in wild-type (Fig. 7c).

Flooding and hypoxia trigger Ca^{2+} changes in both wild-type and *cax2* mutants

CAX2 is a vacuolar ion transporter that would be predicted to play a role in curtailing any elevated cytosolic Ca^{2+} change. Therefore, we directly monitored cytosolic Ca^{2+} levels during flooding and hypoxic stress in wild-type, *cax2-2,* and *cax2-3* plants expressing the GFP-based Ca^{2+} sensor YCNano-65. Fig. 8 and Video S6 show that YCNano-65 reported similar Ca^{2+} elevations in the root to R-GECO (Fig. 1) in wild-type plants providing a robust baseline response to compare mutant dynamics against. Although Ca^{2+} increases were evident upon flooding in the root meristematic and elongation zones in all the genotypes studied, these changes were larger in the *cax2* mutants, consistent with the relatively high *CAX2* expression in the root meristem and into the elongation zone reported by the eFP Browser (Toufighi *et al.*, 2005). In addition, the *cax2* plants showed a slower rate of resetting these Ca^{2+} increases back to prestimulation levels (Fig. 8).

We next asked whether these changes in Ca^{2+} were related to the reduced O_2 levels imposed by our flooding treatment or to some other factor. We therefore developed a custom sample chamber which we could perfuse with N_2(g) and so control the O_2 levels (Fig. S3). In response to this treatment, the root apex and meristematic zone developed a rapid increase in Ca^{2+} that was larger in the *cax2-2* and *cax2-3* mutants than in wild-type seedlings (Figs 9, S6, S7; Video S8). These experiments indicated that the O_2 levels had to drop from *c.* 21% of ambient air to *c.* < 8% in both wild-type and *cax2* mutant before Ca^{2+} increases were triggered. Fig. 8 shows Ca^{2+} data that are normalized to the

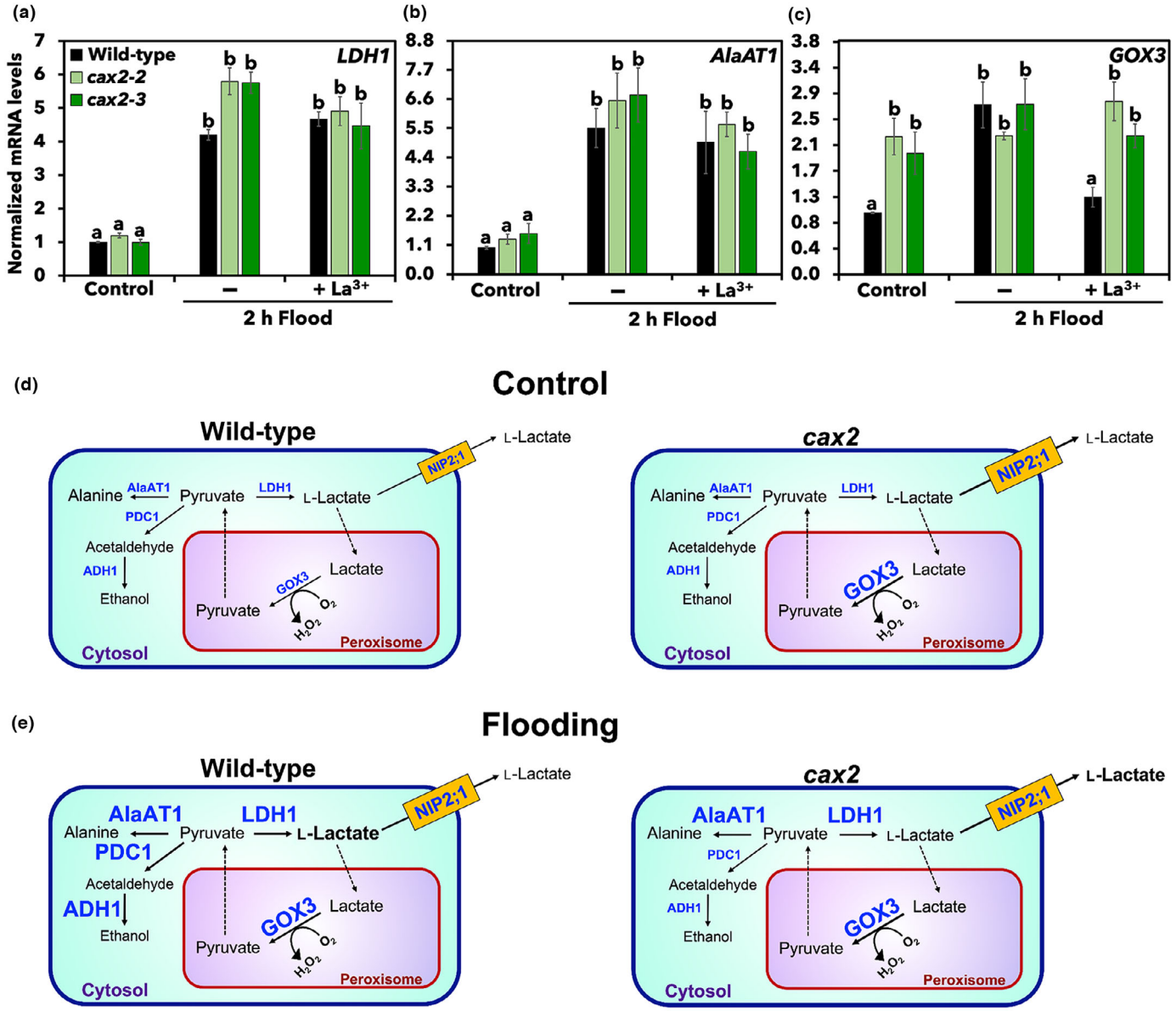

Fig. 7 Loss of *CAX2* function in *Arabidopsis thaliana* affects the expression of pyruvate and lactate metabolizing enzymes. The transcript levels of *LDH1* (a), *AlaAT1* (b), and *GOX3* (c) were analyzed with real-time quantitative polymerase chain reaction (qPCR) in response to 2 h flooding stress with or without prior 1 h La^{3+} pretreatment as described in Fig. 2. Data represent mean ± SE for three to four independent biological replicates. Bars sharing the same letter are not significantly different from each other (one-way ANOVA and Tukey's multiple comparisons test, $P < 0.05$). *LDH1*, *LACTATE DEHYDROGENASE 1*; *AlaAT1*, *ALANINE AMINOTRANSFERASE 1*; *GOX3*, *GLYCOLATE OXIDASE 3*. (d, e) Model displaying pathways involved in the metabolism of pyruvate and lactate in wild-type and *cax2* knockout plants under nonflooded (d) and flooded (e) conditions. Larger size of gene name reflects upregulation. In the absence of *CAX2*, cellular L-lactate levels are removed and recycled faster by the constitutive activation of *NIP2;1*, and *GOX3* as compared to wild-type plants. *CAX2*, *CATION EXCHANGER 2*; *NODULIN26-LIKE INTRINSIC PROTEIN 2;1*.

prestimulation signal to help more easily make comparisons between the dynamics of responses. However, Figs 9 and S5 are presented as non-normalized data which allows comparisons of absolute Ca^{2+} levels. For comparison, Fig. S7 shows the same data as in Fig. 9 but as normalized values and also provides average measurements of resting levels (before hypoxic treatment) and magnitude of peak response. These results show that the resting Ca^{2+} (i.e. before treatment) in *cax2* plants is significantly elevated relative to the wild-type, as is the amplitude of the maximal response.

Consistent with a model where the elevated resting Ca^{2+} in *cax2* could lead to the constitutive upregulation of flood response elements such as *NIP2;1*, *SUS1*, and *GOX3* (Fig. 6f,g), induction of all three of these genes was found to be Ca^{2+}-responsive in wild-type plants, with their transcriptional upregulation by flooding being inhibited by pretreatment with La^{3+} (Figs 7, 10). La^{3+} pretreatment did not have any effect on the flooding-triggered induction of *LDH1* or *AlaAT1* (Fig. 7), that is genes that are related to anaerobic metabolism but that are not constitutively upregulated in the *cax2* background.

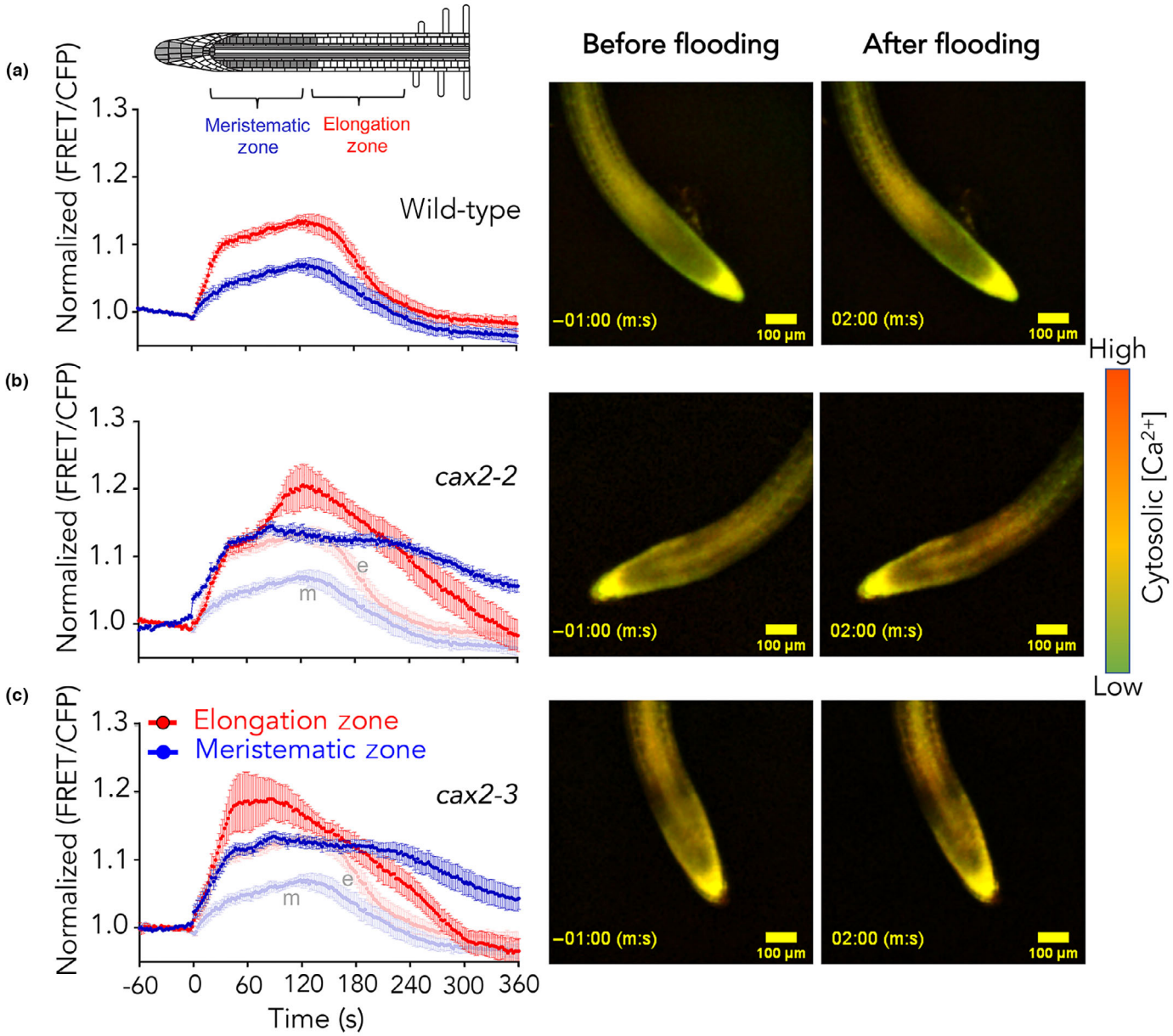

Fig. 8 Flooding triggers Ca^{2+} changes in *Arabidopsis thaliana* wild-type and *cax2* mutant plants. Flooding-triggered Ca^{2+} changes in 7-d-old seedlings of wild-type Col-0 (a), *cax2-2* (b), and *cax2-3* (c) expressing the YCNano-65 GFP-based Ca^{2+} bioreporter. Ca^{2+} changes are indicated as changes in the ratio of FRET : CFP fluorescence from the YCNano-65 reporter monitored in the meristematic and elongation zones, as shown inset in (a). Traces are normalized to the respective prestimulation values for each genotype. Representative images of before and after flooding are shown on the right side of the corresponding graph (right panels of (a–c), taken from Supporting Information Videos S1–S8). Wild-type data from meristematic region (m) and elongation zone (e) taken from (a) is reproduced in (b) and (c) to aid in comparisons. Data are mean ± SEM, $n = 6$. See Videos S5–S7 for representative flooding responses of WT, *cax2-2,* and *cax2-3* used to extract the quantitative data in (a–c). FRET, fluorescence resonance energy transfer; CFP, cyan fluorescent protein.

Discussion

Transcriptome analyses of Arabidopsis experiencing a low O_2 environment have shown that as many as 2000 genes may be either significantly up- or downregulated by such treatments (e.g., Branco-Price *et al.*, 2005, 2008; Liu *et al.*, 2005; Loreti *et al.*, 2005; Baena-González *et al.*, 2007; van Dongen *et al.*, 2009; Mustroph *et al.*, 2010; Licausi *et al.*, 2011). These transcriptional fingerprints have proven extremely powerful tools for researchers to dissect the networks of responses that low O_2 elicits in the plant (reviewed in Bailey-Serres & Voesenek, 2010; Blokhina *et al.*, 2014; Fukao *et al.*, 2019).

Our upregulated Ca^{2+}-related transcriptional response network derived from this analysis included 4 Ca^{2+}-dependent protein kinases (CPKs 2, 23, 28, and 32). In rice, the activity of the Ca^{2+}-regulated kinase OsCIPK15 has been shown to be linked to control of the expression of hypoxic response genes such as *ADH1* (Lee *et al.*, 2009; Meyer *et al.*, 2010). OsCIPK15 may

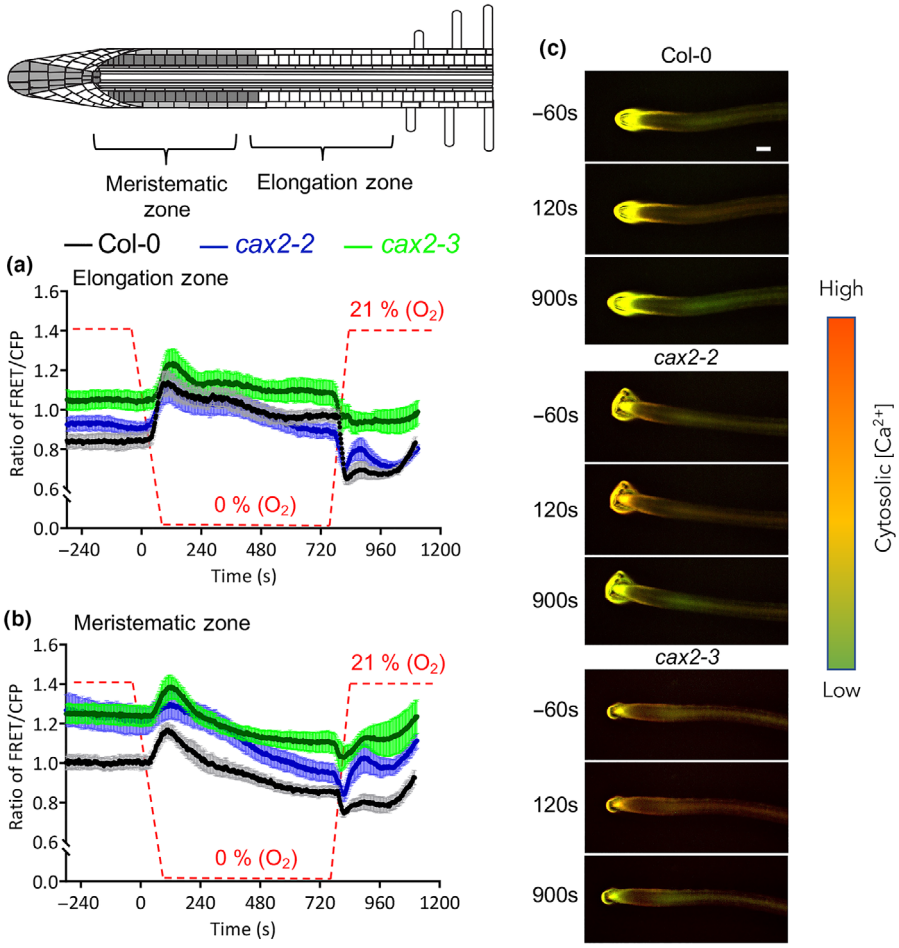

Fig. 9 Ca^{2+} changes are elicited in different developmental zones of the *Arabidopsis thaliana* root to reduced O_2. The Ca^{2+} levels in roots of 7-d-old Col-0, *cax2-2*, or *cax2-3* seedlings were monitored by ratio imaging of plants expressing the GFP-based Ca^{2+} sensor YCNano-65 as O_2 levels were changed. Data are mean ± SEM, $n = 6$. Ca^{2+} changes in the elongation zone (a) and meristem (b). (c) Representative images of the roots of the data in (a, b) for the time frames indicated. N_2(g) was introduced at 0 s. Bar, 200 µm. Note this same data is shown in Supporting Information Fig. S7 but plotted as normalized Ratio values. GFP, Green Fluorescent Protein.

itself be regulated by the SnRK1 kinase, providing a potential direct link to the systems that monitor the energy charge of the cell. However, the roles of CPK family members in flooding and hypoxic response in Arabidopsis remain poorly understood. Half of the rapid hypoxia upregulated, Ca^{2+}-related genes we identified encode calmodulin-like (CML) and calmodulin-binding proteins. Ca^{2+} signaling through calmodulins has been proposed to control a wide range of flooding-related events such as anaerobic protein degradation and solute release (Aurisano *et al.*, 1995). CML38 has also recently emerged as likely playing an important role in low O_2 response through its Ca^{2+}-dependent association with stress granules (Lokdarshi *et al.*, 2016). Future studies of the calmodulin and calmodulin-like proteins in low O_2 response signaling is an area with great potential for additional research. Analysis of this Ca^{2+}-related gene network showed functional enrichment for defense-related genes (Fig. 2f), suggesting a point of potential crosstalk between the pathogen defense and flooding response networks of the plant. Indeed, flooding signaling has been proposed to prime subsequent pathogen defense systems (e.g., Hsu *et al.*, 2013), and calmodulin and CML genes have been closely related to defense response networks (e.g., Yuan *et al.*, 2021).

Of the 28 flooding-induced, Ca^{2+}-related genes from our network analysis that we were able to validate as hypoxically induced, *c.* 50% appeared to require a Ca^{2+} signal for their up-regulation (i.e. up-regulation was inhibited by La^{3+} treatment), with *c.* 14% showing inhibition of their induction by the Ca^{2+} signal (induction was enhanced by La^{3+}, Fig. 1). Features such as the amplitude, duration, rise time, rates of resetting and repetition of Ca^{2+} changes (the 'Ca^{2+} signature' of a stimulus; Dodd *et al.*, 2010) have been shown to be capable of carrying distinct information linked to the modulation of specific transcriptional responses (Whalley & Knight, 2013; Lenzoni *et al.*, 2018; Liu *et al.*, 2020). Thus, responses to distinct elements of a hypoxic Ca^{2+} signature could provide a mechanism whereby a single hypoxic Ca^{2+} signal could lead to complex patterns of gene up- and downregulation. It is also important to note that for this study, our knockout approach to functional characterization led us to focus on upregulated differentially expressed genes. However, genes showing flooding-triggered repression of expression might equally play key regulatory roles in plant flooding responses and their analysis will likely be a fruitful area for future research.

Our analyses highlighted the transcription of two Ca^{2+} transporters, *ACA1* and *CAX2* as being rapidly responsive to hypoxic challenges. ACA1 is found in the ER (Dunkley *et al.*, 2006; Ishka *et al.*, 2021) and CAX2 is a member of the vacuolar cation exchanger family of cation/H^+ antiporters (Pittman *et al.*, 2004).

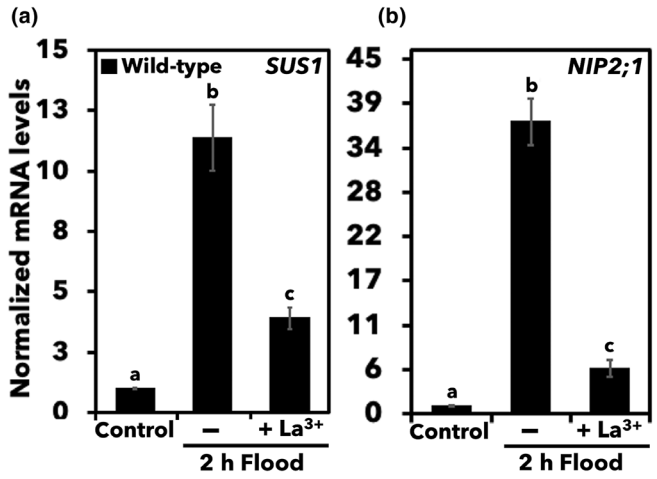

Fig. 10 La^{3+} pretreatment reduces *SUS1* and *NIP2;1* expression in *Arabidopsis thaliana*. The transcript levels of *SUS1* (a) and *NIP2;1* (b) were analyzed with real-time quantitative polymerase chain reaction (qPCR) in response to 2 h flooding stress with or without prior 1 h La^{3+} pretreatment as described in Fig. 2. Data represent mean ± SE for three to four independent biological replicates. Bars sharing the same letter are not significantly different from each other (one-way ANOVA and Tukey's multiple comparisons test, $P < 0.05$). *SUS1*, *SUCROSE SYNTHASE 1*; *NIP2;1*, *NODULIN26-LIKE INTRINSIC PROTEIN 2;1*.

In many of our assays, *aca1-1* behaved like wild-type to flooding stress, such as in flooding-induced reduction in photosynthetic pigments, the elevation of anthocyanin production, and in the qualitative patterns of the upregulation of several stress-related genes (Figs 4, 5). However, mutants in *ACA1* did show reduced induction of hypoxic marker genes. These observations suggest that ACA1 and ER Ca^{2+} transport does likely play a role in hypoxic signaling and response. Indeed, the ER is known to harbor many Ca^{2+}-dependent processes that are likely affected by hypoxia-triggered changes in ER Ca^{2+} dynamics (e.g., Groenendyk *et al.*, 2021). For example, hypoxia-induced ER stress and upregulation of the unfolded protein response may be an important factor across eukaryotes (Bartoszewska & Collawn, 2020) and plants are well documented to show hypoxic effects on features ranging from ER redox dynamics (Ugalde *et al.*, 2022), to triggering the release of hypoxia-related transcription factors sequestered at the ER surface (Eysholdt-Derzsó *et al.*, 2023). However, mutants in *CAX2* were resistant to sustained flooding stress in all the responses we tested, ranging from maintained chlorophyll and carotenoid levels (Fig. 4a) to exhibit no upregulation of a suite of hypoxic stress response genes upon flooding (Figs 5, 6). Taken together, these results imply an important influence of this tonoplast transporter on flooding-related signaling and/or response. CAX2 is thought to have a broad specificity, transporting a range of cations including Ca^{2+}, Mn^{2+} and Cd^{2+} into the vacuole (Hirschi *et al.*, 2000) but its physiological functions have yet to be studied in depth.

CAX2 could directly exert its effects on flooding responses by helping shape the duration and amplitude of cytosolic Ca^{2+} signals. Indeed, modeling of the Ca^{2+} changes linked to defense-related transcriptional responses in Arabidopsis has shown that the falling phase of the Ca^{2+} signature appears to have important, quantitative regulatory action on Ca^{2+}-dependent transcriptional networks (Lenzoni *et al.*, 2018). Fig. 8 indicates that knockout of *CAX2* does lead to elevated and prolonged flooding/hypoxia-triggered Ca^{2+} signals, but in both the wild-type and *cax2* mutant, O_2 levels are required to fall to *c.* < 8% to trigger a Ca^{2+} signal (Figs 9, S6, S7). This threshold broadly agrees with that found for the induction of large-scale molecular responses as O_2 levels are lowered in the literature (e.g., Licausi *et al.*, 2011). The fact that the threshold to trigger Ca^{2+} response is similar in both wild-type and *cax2* mutants is consistent with a model where *CAX2* plays a role downstream of initial O_2 sensing events. However, although the *cax2* mutants show prolonged flooding-induced Ca^{2+} signals (Fig. 8), the sustained elevated Ca^{2+} responses seen upon anoxic treatment returned to basal levels with similar kinetics in both wild-type and *cax2* backgrounds upon return to 21% oxygen (Figs 9, S6, S7). This observation suggests that other factors than only lowered O_2 levels may be affecting Ca^{2+} signal dynamics in the flooding response and that other Ca^{2+} transport systems may be acting in concert with CAX2 to shape these individual responses.

Flooding induction of *ACA1* was enhanced in the *cax2* background by *c.* one-third and *CAX1* expression was constitutively upregulated by *c.* twofold (Fig. S4). The degree to which such changes in these other transporters contribute to the *cax2* phenotype remains to be determined. However, increases in *CAX1* and *ACA1* might be expected to translate to attenuated Ca^{2+} increases rather than the enhanced Ca^{2+} signals seen in the *cax2* background. Knockout of *CAX1* (and *CAX3*) has recently been shown to lead to resistance to the stresses of reoxygenation after anoxic stress and submergence. However, *CAX1* knockouts are not resistant to waterlogging (Yang *et al.*, 2022). Thus, although the CAX family of transporters appears to be important elements in a suite of responses to flooding, specific members may be acting in the response pathways to different components of this stress. Future studies using multiple mutants in the CAXs and ACAs should provide important additional insights into these processes.

Three other Ca^{2+} transporters, *CAX4*, *ACA8*, and *ACA11* have been reported to show reduced expression in response to waterlogging but mutants in these genes exhibited small effects on flooding sensitivity (Wang *et al.*, 2016). A further transporter, CCX5 (originally named *CAX11*), was also downregulated and showed an increase in waterlogging-linked whole plant Ca^{2+} accumulation that may be related to the mutant's hypersensitivity to this stress (Wang *et al.*, 2016). CCX5 belongs to the Arabidopsis calcium cation exchanger superfamily (Shigaki *et al.*, 2006) and likely transports K^+ and Na^+ (Zhang *et al.*, 2011). Precisely how CCX5 exerts such a large influence on Ca^{2+} transport and its relationship to CAX2 remains to be defined.

The Ca^{2+} transport activities of CAX2 are powered by the H^+ gradient across the tonoplast and transcripts for the H^+ pumping vacuolar pyrophosphatase are also increased upon hypoxic challenges (Liu *et al.*, 2010). This parallel regulation of transporters may allow a coordinated increase in vacuolar transport capacity as part of hypoxic signaling and response. Indeed, the vacuole has long been recognized as an important hub for signaling in the

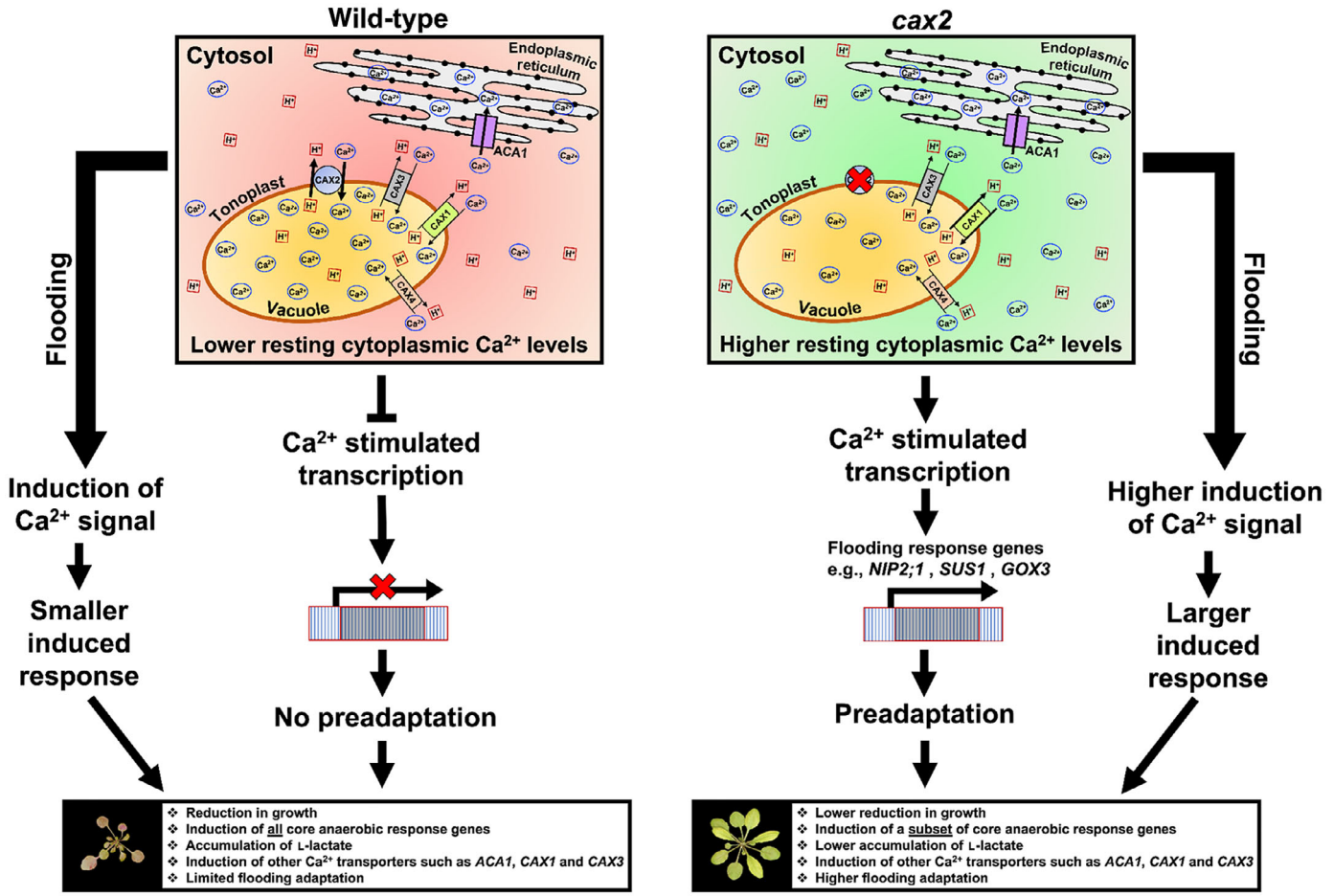

Fig. 11 Proposed involvement of CAX2 in the regulation of flooding-induced low-oxygen stress responses in *Arabidopsis*. CAX2 is a vacuolar ion transporter, which plays a key role in shaping Ca^{2+} signals in the cytoplasm by pumping Ca^{2+} ions into the vacuole and hence both maintain resting Ca^{2+} homeostasis in plant cells and attenuate Ca^{2+} signals once they are generated. Other Ca^{2+} transporters such as ACA1 and other CAX family members (particularly CAX1 and CAX3) also contribute to the removal of Ca^{2+} ions from cytoplasm into the respective cellular compartments. Flooding results in increased levels of *ACA1* and *CAX1* transcripts in both wild-type and *cax2* mutant plants. In addition, knocking out *CAX2* leads to slightly elevated resting Ca^{2+} levels and larger flooding-induced Ca^{2+} signals as compared to the wild-type plants, which suggests a key role of CAX2 in Ca^{2+} removal from cytoplasm into the vacuole. The elevated basal levels may trigger some Ca^{2+}-responsive flooding response elements, such as transcriptional upregulation of *SUS1*, *NIP2;1,* and *GOX3* to be constitutively activated, potentially preadapting the plant to flooding stress. The larger flooding-triggered Ca^{2+} signal generated in *CAX2* knockouts may combine with this effect, causing greater flooding responses in Ca^{2+} responsive elements and so further contributing to flood tolerance. *ACA1*, *AUTOINHIBITED* Ca^{2+} *ATPASE 1*; *CAX1*, *CATION EXCHANGER 1*; *CAX2*, *CATION EXCHANGER 2*; *CAX3*, *CATION EXCHANGER 3*; *SUS1*, *SUCROSE SYNTHASE 1*; *NIP2;1*, *NODULIN26-LIKE INTRINSIC PROTEIN 2;1*; and *GOX3*, *GLYCOLATE OXIDASE 3*.

plant cell (Peiter, 2011). For example, the vacuolar Ca^{2+} ATPases ACA4 and ACA11 likely act as key elements in bacterial defense through their effects on Ca^{2+} signaling dynamics (Hilleary *et al.*, 2020). However, other organelles, such as the mitochondrion (e.g., Subbaiah *et al.*, 1998) and ER (this study), are also likely important elements in shaping plant hypoxia and flooding-related Ca^{2+} signals. For example, the MITOCHONDRIAL Ca^{2+} UNIPORTER (MCU) proteins regulate the Ca^{2+} transport into the mitochondria and the triple mutant *mcu123* seedlings showed no significant differences in calcium accumulation in both cytosol and mitochondrial matrix as compared to wild-type upon hypoxia stress (Ruberti *et al.*, 2022). Conducting future studies to detect calcium changes in these other cellular organelles will be an important avenue to explore their roles in shaping Ca^{2+} signals triggered by flooding and hypoxic stresses.

Knocking out *CAX2* shifted resting Ca^{2+} upward (Fig. 9), an effect also reported for knockouts in the vacuolar and ER Ca^{2+} ATPases (Hilleary *et al.*, 2020; Ishka *et al.*, 2021). This observation leads to a possible explanation for the flooding resistance of the *cax2* mutants as shown in Fig. 11. In the *cax2* background there is an elevated basal level of cytosolic Ca^{2+} that may shift the resting state of the hypoxia/flooding signaling system toward constitutive activation of the more readily Ca^{2+}-activated components of the normal response network. Such preactivation might make the plants better able to cope with the onset of flooding stress (Fig. 11). The *cax2* mutant's larger and prolonged flooding-triggered Ca^{2+} signal would then provide an additional level of subsequent response. This idea of being 'preadapted' to flooding is consistent with the constitutive upregulation in the *cax2* knockouts of some flooding response genes that are closely

linked to anaerobic metabolism such as *SUS1*, *NIP2;1* and *GOX3* (Figs 6, 7). For example, sucrose synthases catalyze the reversible conversion of sucrose and uridine diphosphate (UDP) into UDP-glucose and fructose, and it is thought that the hypoxia-induced shift to sucrose catabolism in flooded plants is dependent on sucrose synthase activity under sugar limiting conditions (Bieniawska *et al.*, 2007; Santaniello *et al.*, 2014).

Similarly, *NIP2;1* has been shown to be an important player in hypoxic response, with knockout mutants exhibiting a lowered ability to survive in response to flooding and low-oxygen conditions (Beamer *et al.*, 2021). In the root, NIP2;1 transports lactic acid to the apoplast/rhizosphere and its knockout mutants have increased lactate levels (Choi & Roberts, 2007; Beamer *et al.*, 2021). Constitutive activation of *NIP2;1* (and *GOX3*) therefore provides a possible explanation for the lower accumulation of cellular L-lactate levels in *cax2* mutant through a combination of both rapid removal (NIP2;1) and recycling to pyruvate in the peroxisome (GOX3). In addition, flooded *cax2* mutants are expected to show less ethanolic fermentation than wild-type as *cax2* shows no flooding-triggered induction of *ADH1* and *PDC1* (Fig. 6a,b). Reduced flux through this pathway would be expected to both reduce carbon loss (as CO_2) and lower the accumulation of cytotoxic ethanol. When coupled with increased carbon sequestration into alanine (upregulation of *AlaAT1*; Diab & Limami, 2016), this suite of biochemical responses might then help protect cellular functions during flooding stress in the *cax2* mutant (Fig. 7e). Additionally, the enhanced amplitude of hypoxia and flooding triggered Ca^{2+} signals (Figs 8, 9) may further enhance the level of other Ca^{2+}-dependent flooding responses in the *cax2* mutant lines. Such shifts in baseline resting Ca^{2+} and larger stimulus-triggered Ca^{2+} signals will likely affect a wide range of processes and so an additional key question for future research is whether *cax2* phenotypes extend to other biotic and abiotic stresses.

Overall, our results indicate that CAX2 is part of the regulatory network that modulates the dynamics of flood-triggered Ca^{2+} signals that are part of a rapid stress response system triggered at the onset of flooding. Further *CAX2* (and *CAX3*) expression is itself induced by flooding, suggesting the plant may be rewiring these signaling networks to play roles in later stages of the response.

It is also important to note that although we have focused on transcription and biochemical pathways as a readout of flooding response in the models shown in Figs 7 and 11, an extensive network of cellular events is known to be triggered by this stress. For example, responses as diverse as shifts in the translatome (Mustroph *et al.*, 2010), generation of signals such as reactive oxygen species (Pucciariello & Perata, 2021), and production of stress granules (Lokdarshi *et al.*, 2016) are all associated with hypoxic challenge. These processes themselves may be linked to Ca^{2+} signaling. Thus, we likely have only scratched the surface of the network of influences Ca^{2+} and CAX2 likely exert on the flooding response network. In addition, although the flooding-triggered Ca^{2+} signals we detected in the roots were stronger than in the shoots (e.g., Fig. 1; Video S3), our biochemical and qPCR analyses in Figs 3–5 of leaf tissues indicate that systemic signals must be being exported from the roots. Defining these mobile signals and their relationship to Ca^{2+} is an additional important challenge for future work.

Acknowledgements

We thank Dr Sarah Swanson, for critical reading of the manuscript and Amanda Miller for invaluable technical assistance. Supported by NSF (NSF IOS1557899, MCB2016177), NASA (NNX14AT25G, 80NSSC19K0126 and 80NSSC21K0577), and USDA Hatch (NEV00389). Confocal imaging was performed at the Newcomb Imaging Center, University of Wisconsin – Madison.

Competing interests

None declared.

Author contributions

AB, WG-C, and SG planned and designed the research. AB, WG-C, SH-K, and SG designed, performed, and analyzed experiments and wrote and edited the manuscript. AB and W-GC contributed equally to this work.

ORCID

Arkadipta Bakshi https://orcid.org/0000-0003-1644-360X
Won-Gyu Choi https://orcid.org/0000-0002-0113-9376
Simon Gilroy https://orcid.org/0000-0001-9597-6839
Su-Hwa Kim https://orcid.org/0000-0002-3008-4562

Data availability

All study data are included in the article or the Supporting Information.

References

Aurisano N, Bertani A, Reggiani R. 1995. Involvement of calcium and calmodulin in protein and amino acid metabolism in rice roots under anoxia. *Plant and Cell Physiology* **36**: 1525–1529.

Baena-González E, Rolland F, Thevelein JM, Sheen J. 2007. A central integrator of transcription networks in plant stress and energy signalling. *Nature* **448**: 938–942.

Bailey-Serres J, Chang R. 2005. Sensing and signalling in response to oxygen deprivation in plants and other organisms. *Annals of Botany* **96**: 507–518.

Bailey-Serres J, Voesenek LACJ. 2008. Flooding stress: acclimations and genetic diversity. *Annual Review of Plant Biology* **59**: 313–339.

Bailey-Serres J, Voesenek LACJ. 2010. Life in the balance: a signaling network controlling survival of flooding. *Current Opinion in Plant Biology* **13**: 489–494.

Bakshi A, Gilroy S. 2023. Analysis of plant flooding response. *Methods in Enzymology* **680**: 461–491.

Bartoszewska S, Collawn JF. 2020. Unfolded protein response (UPR) integrated signaling networks determine cell fate during hypoxia. *Cellular & Molecular Biology Letters* **25**: 18.

Beamer ZG, Routray P, Choi W-G, Spangler MK, Lokdarshi A, Roberts DM. 2021. Aquaporin family lactic acid channel NIP2;1 promotes plant survival under low oxygen stress in Arabidopsis. *Plant Physiology* **187**: 2262–2278.

Bergmeyer HU, Bernt E. 1974. UV-Assay with pyruvate and NADH. In: Bergmeyer HU, ed. *Methods of enzymatic analysis*. New York, NY, USA: Academic Press, 574–579.

Bieniawska Z, Paul Barratt DH, Garlick AP, Thole V, Kruger NJ, Martin C, Zrenner R, Smith AM. 2007. Analysis of the sucrose synthase gene family in Arabidopsis. *The Plant Journal* **49**: 810–828.

Blokhina OB, Törönen P, Fagerstedt KV. 2014. Oxidative stress components explored in anoxic and hypoxic global gene expression data. *Plant Cell Monographs* **21**: 19–39.

Boudsocq M, Sheen J. 2010. Stress signaling II: calcium sensing and signaling. In: Pareek A, Sopory SK, Bohrnert HJ, eds. *Abiotic stress adaptation in plants*. Dordrecht, the Netherlands: Springer, 75–90.

Branco-Price C, Kaiser KA, Jang CJH, Larive CK, Bailey-Serres J. 2008. Selective mRNA translation coordinates energetic and metabolic adjustments to cellular oxygen deprivation and reoxygenation in *Arabidopsis thaliana*. *The Plant Journal* **56**: 743–755.

Branco-Price C, Kawaguchi R, Ferreira RB, Bailey-Serres J. 2005. Genome-wide analysis of transcript abundance and translation in Arabidopsis seedlings subjected to oxygen deprivation. *Annals of Botany* **96**: 647–660.

Choi WG, Barker RJ, Kim SH, Swanson SJ, Gilroy S. 2019. Variation in the transcriptome of different ecotypes of *Arabidopsis thaliana* reveals signatures of oxidative stress in plant responses to spaceflight. *American Journal of Botany* **106**: 123–136.

Choi WG, Roberts DM. 2007. Arabidopsis NIP2;1, a major intrinsic protein transporter of lactic acid induced by anoxic stress. *Journal of Biological Chemistry* **282**: 24209–24218.

Choi W-G, Toyota M, Kim S-H, Hilleary R, Gilroy S. 2014. Salt stress-induced Ca^{2+} waves are associated with rapid, long-distance root-to-shoot signaling in plants. *Proceedings of the National Academy of Sciences, USA* **111**: 6497–6502.

Chung HJ, Ferl RJ. 1999. Arabidopsis alcohol dehydrogenase expression in both shoots and roots is conditioned by root growth environment. *Plant Physiology* **121**: 429–436.

Diab H, Limami AM. 2016. Reconfiguration of N metabolism upon hypoxia stress and recovery: roles of alanine aminotransferase (AlaAT) and glutamate dehydrogenase (GDH). *Plants* **5**: 25.

Dodd AN, Kudla J, Sanders D. 2010. The language of calcium signaling. *Annual Review of Plant Biology* **61**: 593–620.

Dolferus R, Wolansky M, Carroll R, Miyashita Y, Ismond K, Good A. 2008. Functional analysis of lactate dehydrogenase during hypoxic stress in *Arabidopsis*. *Functional Plant Biology* **35**: 131–140.

van Dongen JT, Fröhlich A, Ramírez-Aguilar SJ, Schauer N, Fernie AR, Erban A, Kopka J, Clark J, Langer A, Geigenberger P. 2009. Transcript and metabolite profiling of the adaptive response to mild decreases in oxygen concentration in the roots of Arabidopsis plants. *Annals of Botany* **103**: 269–280.

Dunkley TPJ, Hester S, Shadforth IP, Runions J, Weimar T, Hanton SL, Griffin JL, Bessant C, Brandizzi F, Hawes C *et al.* 2006. Mapping the Arabidopsis organelle proteome. *Proceedings of the National Academy of Sciences, USA* **103**: 6518–6523.

Engqvist MK, Schmitz J, Gertzmann A, Florian A, Jaspert N, Arif M, Balazadeh S, Mueller-Roeber B, Fernie AR, Maurino VG. 2015. GLYCOLATE OXIDASE3, a glycolate oxidase homolog of yeast L-lactate cytochrome c oxidoreductase, supports L-lactate oxidation in roots of Arabidopsis. *Plant Physiology* **169**: 1042–1061.

Eysholdt-Derzsó E, Renziehausen T, Frings S, Frohn S, von Bongartz K, Igisch CP, Mann J, Häger L, Macholl J, Leisse D *et al.* 2023. Endoplasmic reticulum-bound ANAC013 factor is cleaved by RHOMBOID-LIKE 2 during the initial response to hypoxia in *Arabidopsis thaliana*. *Proceedings of the National Academy of Sciences, USA* **120**: e2221308120.

Fukao T, Barrera-Figueroa BE, Juntawong P, Peña-Castro JM. 2019. Submergence and waterlogging stress in plants: a review highlighting research opportunities and understudied aspects. *Frontiers in Plant Science* **10**: 340.

Greenway H, Gibbs J. 2003. Review: Mechanisms of anoxia tolerance in plants. II. Energy requirements for maintenance and energy distribution to essential processes. *Functional Plant Biology* **30**: 999–1036.

Groenendyk J, Agellon LB, Michalak M. 2021. Calcium signaling and endoplasmic reticulum stress. *International Review of Cell and Molecular Biology* **363**: 1–20.

Hilleary R, Paez-Valencia J, Vens C, Toyota M, Palmgren M, Gilroy S. 2020. Tonoplast-localized Ca^{2+} pumps regulate Ca^{2+} signals during pattern-triggered immunity in *Arabidopsis thaliana*. *Proceedings of the National Academy of Sciences, USA* **117**: 18849–18857.

Hirschi KD, Korenkov VD, Wilganowski NL, Wagner GJ. 2000. Expression of Arabidopsis *CAX2* in tobacco. Altered metal accumulation and increased manganese tolerance. *Plant Physiology* **124**: 125–133.

Horikawa K, Yamada Y, Matsuda T, Kobayashi K, Hashimoto M, Matsu-ura T, Miyawaki A, Michikawa T, Mikoshiba K, Nagai T. 2010. Spontaneous network activity visualized by ultrasensitive Ca^{2+} indicators, yellow Cameleon-Nano. *Nature Methods* **7**: 729–732.

Hsu FC, Chou MY, Chou SJ, Li YR, Peng HP, Shih MC. 2013. Submergence confers immunity mediated by the WRKY22 transcription factor in Arabidopsis. *Plant Cell* **25**: 2699–2713.

Igamberdiev AU, Hill RD. 2018. Elevation of cytosolic Ca^{2+} in response to energy deficiency in plants: the general mechanism of adaptation to low oxygen stress. *The Biochemical Journal* **475**: 1411–1425.

Ishka MR, Brown E, Rosenberg A, Romanowsky S, Davis JA, Choi WG, Harper JF. 2021. Arabidopsis Ca^{2+}-ATPases 1, 2, and 7 in the endoplasmic reticulum contribute to growth and pollen fitness. *Plant Physiology* **185**: 1966–1985.

Keinath NF, Waadt R, Brugman R, Schroeder JI, Grossmann G, Schumacher K, Krebs M. 2015. Live cell imaging with R-GECO1 sheds light on flg22- and chitin-induced transient [Ca^{2+}]cyt patterns in Arabidopsis. *Molecular Plant* **8**: 1188–1200.

Lee KW, Chen PW, Lu CA, Chen S, David Ho TH, Yu SM. 2009. Coordinated responses to oxygen and sugar deficiency allow rice seedlings to tolerate flooding. *Science Signaling* **2**: ra61.

Lenzoni G, Liu J, Knight MR. 2018. Predicting plant immunity gene expression by identifying the decoding mechanism of calcium signatures. *New Phytologist* **217**: 1598–1609.

Lewis BD, Spalding EP. 1998. Nonselective block by La^{3+} of Arabidopsis ion channels involved in signal transduction. *Journal of Membrane Biology* **162**: 81–90.

Li S, Wang W, Gao J, Yin K, Wang R, Wang C, Petersen M, Mundy J, Qiu JL. 2016. MYB75 phosphorylation by MPK4 is required for light-induced anthocyanin accumulation in Arabidopsis. *Plant Cell* **28**: 2866–2883.

Licausi F, Weits DA, Pant BD, Scheible WR, Geigenberger P, van Dongen JT. 2011. Hypoxia responsive gene expression is mediated by various subsets of transcription factors and miRNAs that are determined by the actual oxygen availability. *New Phytologist* **190**: 442–456.

Lin BL, Wang JS, Liu HC, Chen RW, Meyer Y, Barakat A, Delseny M. 2001. Genomic analysis of the Hsp70 superfamily in *Arabidopsis thaliana*. *Cell Stress & Chaperones* **6**: 201–208.

Liu F, Vantoai T, Moy LP, Bock G, Linford LD, Quackenbush J. 2005. Global transcription profiling reveals comprehensive insights into hypoxic response in Arabidopsis. *Plant Physiology* **137**: 1115–1129.

Liu J, Lenzoni G, Knight MR. 2020. Design principle for decoding calcium signals to generate specific gene expression via transcription. *Plant Physiology* **182**: 1743–1761.

Liu Q, Zhang Q, Burton RA, Shirley NJ, Atwell BJ. 2010. Expression of vacuolar H^+-pyrophosphatase (OVP3) is under control of an anoxia-inducible promoter in rice. *Plant Molecular Biology* **72**: 47–60.

Lokdarshi A, Craig Conner W, McClintock C, Li T, Roberts DM. 2016. Arabidopsis CML38, a calcium sensor that localizes to ribonucleoprotein complexes under hypoxia stress. *Plant Physiology* **170**: 1046–1059.

Loreti E, Poggi A, Novi G, Alpi A, Perata P. 2005. A genome-wide analysis of the effects of sucrose on gene expression in Arabidopsis seedlings under anoxia. *Plant Physiology* **137**: 1130–1138.

McCormack E, Tsai YC, Braam J. 2005. Handling calcium signaling: Arabidopsis CaMs and CMLs. *Trends in Plant Science* **10**: 383–389.

Meyer AK, Longin CFH, Klose C, Hermann A. 2010. New regulator for energy signaling pathway in plants highlights conservation among species. *Science Signaling* **3**: jc5.

Mithran M, Paparelli E, Novi G, Perata P, Loreti E. 2014. Analysis of the role of the pyruvate decarboxylase gene family in *Arabidopsis thaliana* under low-oxygen conditions. *Plant Biology* **16**: 28–34.

Miyashita Y, Dolferus R, Ismond KP, Good AG. 2007. Alanine aminotransferase catalyses the breakdown of alanine after hypoxia in *Arabidopsis thaliana*. *The Plant Journal* **49**: 1108–1121.

Mustroph A, Lee SC, Oosumi T, Zanetti ME, Yang H, Ma K, Yaghoubi-Masihi A, Fukao T, Bailey-Serres J. 2010. Cross-kingdom comparison of transcriptomic adjustments to low-oxygen stress highlights conserved and plant-specific responses. *Plant Physiology* **152**: 1484–1500.

Peiter E. 2011. The plant vacuole: emitter and receiver of calcium signals. *Cell Calcium* **50**: 120–128.

Pittman JK, Shigaki T, Marshall JL, Morris JL, Cheng NH, Hirschi KD. 2004. Functional and regulatory analysis of the *Arabidopsis thaliana* CAX2 cation transporter. *Plant Molecular Biology* **56**: 959–971.

Pucciariello C, Parlanti S, Banti V, Novi G, Perata P. 2012. Reactive oxygen species-driven transcription in Arabidopsis under oxygen deprivation. *Plant Physiology* **159**: 184–196.

Pucciariello C, Perata P. 2021. The oxidative paradox in low oxygen stress in plants. *Antioxidants* **10**: 332.

Ruberti C, Feitosa-Araujo E, Xu Z, Wagner S, Grenzi M, Darwish E, Lichtenauer S, Fuchs P, Parmagnani AS, Balcerowicz D, *et al.* 2022. MCU proteins dominate in vivo mitochondrial Ca^{2+} uptake in Arabidopsis roots. *Plant Cell* **34**: 4428–4452.

Santaniello A, Loreti E, Gonzali S, Novi G, Perata P. 2014. A reassessment of the role of sucrose synthase in the hypoxic sucrose-ethanol transition in Arabidopsis. *Plant, Cell & Environment* **37**: 2294–2302.

Sasidharan R, Hartman S, Liu Z, Martopawiro S, Sajeev N, van Veen H, Yeung E, Voesenek LACJ. 2018. Signal dynamics and interactions during flooding stress. *Plant Physiology* **176**: 1106–1117.

Schindelin J, Arganda-Carreras I, Frise E, Kaynig V, Longair M, Pietzsch T, Preibisch S, Rueden C, Saalfeld S, Schmid B *et al.* 2012. Fiji: an open-source platform for biological-image analysis. *Nature Methods* **9**: 676–682.

Schmidt RR, Weits DA, Feulner CFJ, Van Dongen JT. 2018. Oxygen sensing and integrative stress signaling in plants. *Plant Physiology* **176**: 1131–1142.

Schmittgen TD, Livak KJ. 2008. Analyzing real-time PCR data by the comparative CT method. *Nature Protocols* **3**: 1101–1108.

Sedbrook JC, Kronebusch PJ, Borisy GG, Trewavas AJ, Masson PH. 1996. Transgenic AEQUORIN reveals organ-specific cytosolic Ca^{2+} responses to anoxia in *Arabidopsis thaliana* seedling. *Plant Physiology* **111**: 243–257.

Shigaki T, Rees I, Nakhleh L, Hirschi KD. 2006. Identification of three distinct phylogenetic groups of CAX cation/proton antiporters. *Journal of Molecular Evolution* **63**: 815–825.

Subbaiah CC, Bush DS, Sachs MM. 1994a. Elevation of cytosolic calcium precedes anoxic gene expression in maize suspension-cultured cells. *Plant Cell* **6**: 1747–1762.

Subbaiah CC, Bush DS, Sachs MM. 1998. Mitochondrial contribution to the anoxic Ca^{2+} signal in maize suspension-cultured cells. *Plant Physiology* **118**: 759–771.

Subbaiah CC, Junkai Z, Sachs MM. 1994b. Involvement of intracellular calcium in anaerobic gene expression and survival of maize seedlings. *Plant Physiology* **105**: 369–376.

Thimm O, Bläsing O, Gibon Y, Nagel A, Meyer S, Krüger P, Selbig J, Müller LA, Rhee SY, Stitt M. 2004. MAPMAN: a user-driven tool to display genomics data sets onto diagrams of metabolic pathways and other biological processes. *The Plant Journal* **37**: 914–939.

Toufighi K, Brady SM, Austin R, Ly E, Provart NJ. 2005. The botany array resource: e-Northerns, expression angling, and promoter analyses. *The Plant Journal* **43**: 153–163.

Toyota M, Spencer D, Sawai-Toyota S, Jiaqi W, Zhang T, Koo AJ, Howe GA, Gilroy S. 2018. Glutamate triggers long-distance, calcium-based plant defense signaling. *Science* **361**: 1112–1115.

Tsuji H, Nakazono M, Saisho D, Tsutsumi N, Hirai A. 2000. Transcript levels of the nuclear-encoded respiratory genes in rice decrease by oxygen deprivation: evidence for involvement of calcium in expression of the alternative oxidase 1a gene. *FEBS Letters* **471**: 201–204.

Ugalde JM, Aller I, Kudrjasova L, Schmidt RR, Schlößer M, Homagk M, Fuchs P, Lichtenauer S, Schwarzländer M, Müller-Schüssele SJ *et al.* 2022. Endoplasmic reticulum oxidoreductin provides resilience against reductive stress and hypoxic conditions by mediating luminal redox dynamics. *Plant Cell* **34**: 4007–4027.

Voesenek LACJ, Bailey-Serres J. 2015. Flood adaptive traits and processes: an overview. *New Phytologist* **206**: 57–73.

Wang F, Chen ZH, Liu X, Colmer TD, Zhou M, Shabala S. 2016. Tissue-specific root ion profiling reveals essential roles of the CAX and ACA calcium transport systems in response to hypoxia in Arabidopsis. *Journal of Experimental Botany* **67**: 3747–3762.

Wang F, Chen Z-H, Shabala S. 2017. Hypoxia sensing in plants: on a quest for ion channels as putative oxygen sensors. *Plant & Cell Physiology* **58**: 1126–1142.

Whalley HJ, Knight MR. 2013. Calcium signatures are decoded by plants to give specific gene responses. *New Phytologist* **197**: 690–693.

Yang J, Mathew IE, Rhein H, Barker R, Guo Q, Brunello L, Loreti E, Barkla BJ, Gilroy S, Perata P *et al.* 2022. The vacuolar H^+/Ca transporter CAX1 participates in submergence and anoxia stress responses. *Plant Physiology* **190**: 2617–2636.

Yemelyanov VV, Shishova MF, Chirkova TV, Lindberg SM. 2011. Anoxia-induced elevation of cytosolic Ca^{2+} concentration depends on different Ca^{2+} sources in rice and wheat protoplasts. *Planta* **234**: 271–280.

Yuan P, Tanaka K, Poovaiah BW. 2021. Calcium/calmodulin-mediated defense signaling: what is looming on the horizon for AtSR1/CAMTA3-mediated signaling in plant immunity. *Frontiers in Plant Science* **12**: 795353.

Zhang X, Zhang M, Takano T, Liu S. 2011. Characterization of an AtCCX5 gene from *Arabidopsis thaliana* that involves in high-affinity K^+ uptake and Na^+ transport in yeast. *Biochemical and Biophysical Research Communications* **414**: 96–100.

Zhao Y, Araki S, Wu J, Teramoto T, Chang YF, Nakano M, Abdelfattah AS, Fujiwara M, Ishihara T, Nagai T *et al.* 2011. An expanded palette of genetically encoded Ca^{2+} indicators. *Science* **333**: 1888–1891.

Zhou Y, Zhou B, Pache L, Chang M, Khodabakhshi AH, Tanaseichuk O, Benner C, Chanda SK. 2019. Metascape provides a biologist-oriented resource for the analysis of systems-level datasets. *Nature Communications* **10**: 1523.

Supporting Information

Additional Supporting Information may be found online in the Supporting Information section at the end of the article.

Fig. S1 Characterization of mutants in *ACA1* and *CAX2*.

Fig. S2 Setup for soil waterlogging.

Fig. S3 Custom-built microscopy chamber for controlling O_2 levels in atmosphere around Arabidopsis on confocal microscope stage.

Fig. S4 Flooding induces Ca^{2+} changes in the root apex in response to flooding.

Fig. S5 Expression levels of *ACA1* and other *CAX* family genes in response to flooding.

Fig. S6 Hypoxia induces Ca^{2+} changes in the root apex in Col-0, *cax2-2,* and *cax2-3*.

Fig. S7 Hypoxia induces Ca^{2+} changes in the root apex in Col-0, *cax2-2,* and *cax2-3* shown as normalized data.

Table S1 Primers used in this study.

Table S2 Analysis of publicly available hypoxia/anoxia-related mRNA and polysome microarray datasets.

Table S3 qPCR data for 32 candidate hypoxia/flooding upregulated genes in response to hypoxia.

Video S1 Ca^{2+} changes in root exposed to deoxygenated medium.

Video S2 Lack of Ca^{2+} changes in root exposed to oxygenated medium.

Video S3 Lack of Ca^{2+} changes in shoot exposed to deoxygenated medium.

Video S4 Lack of Ca^{2+} changes in shoot exposed to oxygenated medium.

Video S5 Ca^{2+} changes in the root apex upon flooding in wild-type (Col-0) plants.

Video S6 Ca^{2+} changes in the root apex upon flooding in wild-type *cax2-2* plants.

Video S7 Ca^{2+} changes in the root apex upon flooding in *cax2-3* plants.

Video S8 Ca^{2+} changes in the root apex upon altering ambient O_2 levels in wild-type (Col-0) and *cax2-2* plants.

Please note: Wiley is not responsible for the content or functionality of any Supporting Information supplied by the authors. Any queries (other than missing material) should be directed to the *New Phytologist* Central Office.